# Branched GDGT variability in sediments and soils from catchments with marked temperature seasonality

Min Cao[a,*], Gemma Rueda[a], Pedro Rivas-Ruiz[a], Mª Carmen Trapote[b], Mona Henriksen[c], Teresa Vegas-Vilarrúbia[b,d] and Antoni Rosell-Melé[a,e,†]

[a] Institute of Environmental Science and Technology, Universitat Autònoma de Barcelona, 08193 Bellaterra, Catalonia

[b] Department of Evolutive Biology, Ecology and Environmental Sciences, Universitat de Barcelona, 08028 Barcelona, Catalonia

[c] Faculty of Environmental Sciences and Natural Resource Management, Norwegian University of Life Sciences (NMBU), PO BOX 5003, 1432 Aas, Norway

[d] Catalan Institute of Paleontology Miquel Crusafont, 08028, Catalonia

[e] Institució Catalana de Recerca i Estudis Avançats (ICREA), 08011 Barcelona, Catalonia

*Current address: Key Laboratory of Karst Environment, School of Geographical Sciences, Southwest University, Chongqing, 400715, China. Email: smilecaomina@hotmail.com

[†]corresponding author email: antoni.rosell@uab.cat

# Abstract

The distributions of branched glycerol dialkyl glycerol tetraethers (brGDGTs) in sediments are used as a proxy measurement to infer changes in past mean annual air temperatures (MAT). When applied in high resolution sedimentary sequences, measurement of brGDGT distributions is employed to reconstruct MAT at subdecadal time scales. In addition, brGDGT proxy estimates are also sometimes purported to be seasonally biased in environments where annual brGDGT production may not be constant during a seasonal cycle. The main aim of this study was to assess the occurrence of seasonality in the production and distribution of brGDGTs, and the sesonality bias of the derived temperature proxy. For this purpose, we examined brGDGT distributions and brGDGTs-derived MAT estimates, in surface soils and settling/suspended particulate matter over one year from two sites located in the same latitude but at different altitudes, in the Catalan Pyrenees, as well as at one site in southern Norway. These locations have marked seasonal temperature cycles, which were expected to maximize the possibility of detecting any seasonal bias in the production and compositions of brGDGTs. The results show that brGDGT abundance is heterogeneous and increases with soil humidity. The brGDGT distributions and some of the brGDGT-derived proxy measurements in soils are relatively stable throughout the year and do not change significantly in the suspended particulate matter in the river or settling particulate matter in traps. Our study shows that the impact of the seasonality of temperature on brGDGT distribution was absent in the soils studied, regardless of altitude or latitude on a catchment/regional scale. As soils are likely to contain a brGDGT signature which is representative of average environmental conditions in the catchment at least over decades, brGDGT proxy reconstructions derived from soil sources are more suitable to infer variability in environmental parameters over the same timescales (i.e. decades or longer). On shorter timescales (i.e. annual), sediment downcore variability in brGDGTs is likely to be related to changes derived from *in situ* production and sediment sources.

# 1. Introduction

Branched glycerol dialkyl glycerol tetraethers (brGDGTs; Fig. S1), which contain 4–6 methyl groups and 0-2 cyclopentane rings, are common lipids in terrestrial and aquatic environments. They are thought to originate from heterotrophic bacteria (Weijers et al., 2006, 2010; Sinninghe Damsté et al., 2011) that preferentially grow under suboxic conditions, possibly as facultative aerobic heterotrophs (Ayari et al., 2013; Huguet et al., 2013a; Huguet et al., 2017). However, their phylogeny and habitat diversity remains to be established.

BrGDGTs have been described in peat bogs (Schouten et al., 2000; Weijers et al., 2006; Huguet et al., 2010a, 2013b; Naafs et al., 2017a), soils (Weijers et al., 2007; Sinninghe Damsté et al., 2008; Bendle et al., 2010; Huguet et al., 2010b; Loomis et al., 2011; Menges et al., 2014; Yang et al., 2014a; Warden et al., 2016; Coffinet et al., 2017), stalagmites (Yang et al., 2011; Blyth and Schouten, 2013), water suspended particulate matter (SPM) in continental settings (Blaga et al., 2009, 2011; Bechtel et al., 2010; Fietz et al., 2012; Schoon et al., 2013; Buckles et al., 2014; De Jonge et al., 2014a; Loomis et al., 2014; Hu et al., 2016), river and lake sediments (Blaga et al., 2009; Tierney and Russell, 2009; Zink et al., 2010; Loomis et al., 2011; Sun et al., 2011; Zhang et al., 2012; Shanahan et al., 2013; Ajioka et al., 2014a; Zell et al., 2014a; Hanna et al., 2016; Freymond et al., 2017; Peterse and Eglinton, 2017), windborne particulate matter (Fietz et al., 2013; Weijers et al., 2014), marine coastal (Hopmans et al., 2004; Kim et al., 2009; Rueda et al., 2009; Zhu et al., 2011; Liu et al., 2014; Zell et al., 2014a; French et al., 2015; Hanna et al., 2016; Sinninghe Damsté et al., 2016; Warden et al., 2016) and open ocean settings (Huguet et al., 2008; Fietz et al., 2012; Sparkes et al., 2015; Pan et al., 2016; Yamamoto et al., 2016; Jaeschke et al., 2017).

The global distribution of brGDGTs in soils and peatbogs has been related to both pH and air temperature (Weijers et al., 2007; Peterse et al., 2009a, 2012; Tyler et al., 2010; Naafs et al., 2017b). These environmental influences on brGDGT distributions have been expressed through the measurement of the degree of cyclisation of the brGDGTs, calculated via the so-called CBT index, and the degree of methylation, expressed as the MBT or MBT' indices. The global calibration of these indices yields significantly large errors of about 5.0 °C and 0.8 pH units (Weijers et al., 2007; Peterse et al., 2012), which can be reduced in some regional data sets (Tierney et al., 2010; Loomis et al., 2012; Anderson et al., 2014; Yang et al., 2014b; Wang et al., 2016; Coffinet et al., 2017). The empirical relationship between MBT and air temperature has been further validated by the passive incubation of experimental peatland plots (Huguet et al., 2013b), and the study of soil samples in altitudinal or geothermal gradients (Sinninghe Damsté et al., 2008; Peterse et al., 2009b; Ernst et al., 2013; Liu et al., 2013; Anderson et al., 2014; Deng et al., 2016; Coffinet et al., 2017). Similarly, the CBT vs. pH relationship in soils was confirmed through the study of brGDGT distributions in long term (>45 years) soil pH manipulation plots (Peterse et al., 2010).

Given the temperature and pH dependence of brGDGT indices in soils and peats, they are used as proxies for these parameters in loess-palaeosol, peat and sedimentary records (e.g. Weijers et al., 2007; Schouten et al., 2008; Rueda et al., 2009; Ballantyne et al., 2010; Bendle et al., 2010; Tyler et al., 2010; Fawcett et al., 2011; Peterse et al., 2011; Gao et al., 2012; Niemann et al., 2012; Zech et al., 2012; Ajioka et al., 2014b; Sanchi et al., 2014; Cao et al., 2017; Wang et al., 2017a). However, brGDGTs are also argued to be produced *in situ* within the water column or the sediments of aquatic settings (e.g. Tierney and Russell, 2009; Tierney et al., 2010; Loomis et al., 2011; Buckles et al., 2014). This poses a major challenge or may invalidate the application of the soil brGDGT proxies and their calibration equations in sedimentary environments to reconstruct air temperatures and soil pH. However, in lakes such a drawback is circumvented by the development of regional lacustrine sediment calibrations (Blaga et al., 2010; Tierney et al., 2010; Zink et al., 2010; Pearson et al., 2011; Peterse et al., 2011; Sun et al., 2011; Buckles et al., 2014). In fact, there is also a significant correlation on a global scale of the CBT/MBT proxies in lacustrine sediments with temperature and pH (Sun et al., 2011), but new proxy models are still necessary in order to improve the accuracy and precision of using brGDGT distributions as climatic proxies (Pearson et al., 2011). However, the identity and niche of the source organisms in aquatic settings are still unknown.

In some regional studies, pH and temperature were not the primary variables that explained the spatial distribution of brGDGT indices. Their variability may have been influenced by precipitation, soil properties (texture, humidity), seasonality of production, and/or the use of air rather than soil temperature in the calibrations (Weijers et al., 2007; Peterse et al., 2009a; Rueda et al., 2009; Loomis et al., 2011; Peterse et al., 2011; Sun et al., 2011; Dirghangi et al., 2013; Anderson et al., 2014; Menges et al., 2014; Wang et al., 2014; Dang et al., 2016; Davtian et al., 2016; Lei et al., 2016). Some studies have argued that the original MBT/MBT' and CBT indices, if modified to account for the identification of new brGDGT isomers, might explain some of the scatter in the global calibrations (De Jonge et al., 2014b; Yang et al., 2015; Wang et al., 2016), but this may not hold true universally (Warden et al., 2016). The choice of extraction technique, that recovers different pools of lipids, may also lead to a bias in the observed distributions of brGDGTs (Huguet et al., 2010b; Weber et al., 2017).

The brGDGT palaeo proxies were initially calibrated against annual mean values of environmental parameters. A number of studies have claimed that the proxy estimates are biased towards specific seasons, usually summer mean values (Rueda et al., 2009; Peterse et al., 2011; Shanahan et al., 2013; Wu et al., 2013; Deng et al., 2016; Wang et al., 2016). This hypothesis relies on the assumption that there is a preferential period of bio-production of brGDGT, due to favourable environmental conditions, that might further cause a seasonal bias in the temperature-related membrane lipids in the soils or peats (Huguet et al., 2013b). However, in general, no apparent seasonal pattern in the distribution of either core (C-brGDGTs) or intact polar lipid (I-brGDGTs, i.e., GDGTs bound to 1 or 2 polar head groups) derived brGDGTs has been found in soils, exhibiting no obvious shift towards a particular season (Weijers et al., 2011; Lei et al., 2016). The main argument to explain the lack of seasonality in soil derived signals is the slow turnover time of brGDGTs in soils. This has been estimated to be of ca. 18 y for branched C-GDGTs in arable soils in temperate climates (Weijers et al., 2010), and 8–41 y in peat for C-brGDGTs and 11–14 y for I-brGDGTs, suggesting that brGDGTs turnover is on timescales of decades in terrestrial environments (Huguet et al., 2017). However, even much longer turnover times (320–510 y) were observed in anoxic samples (Huguet et al., 2017).

Few studies have monitored the seasonal variability of brGDGT proxies, by means of the monthly sampling of SPM or settling particles in a trap in lakes (Blaga et al., 2011; Buckles et al., 2014; Loomis et al., 2014) or the ocean (Yamamoto et al., 2016). In general, while the fluxes of brGDGTs are seasonal and coupled to the local climatology, the estimated brGDGT temperatures did not match the monthly instrumental variability in local air or water temperatures. In some instances, the fractional abundances of brGDGTs in settling particles showed little seasonal variability over the sampling period (2-3 years) despite large seasonal changes in the fluxes and the actual air and water temperatures (Loomis et al., 2014; Yamamoto et al., 2016).

In this study, we assessed further the occurrence of seasonality in the production and distribution of C-brGDGTs by undertaking their monthly analysis for over a year in both soils and particulate matters from three different catchments. Two sites were located in mountain environments in the pre-Pyrenees and the Pyrenees, and one site in southern Norway (Fig. 1a). The locations considered all have a marked seasonal temperature cycle, but they afforded different types of particulate matter and soils from catchments of different size and nature, which we expected would maximize the possibility of detecting any seasonal bias in the production and composition of brGDGTs. Thus, the high mountain site in the Pyrenees was chosen to obtain recently formed suspended particulate matter in the runoff collected in ephemeral streams from the spring melting of the seasonal snow cover on a small catchment overlapping a former glacier cirque. The Norwegian site, in contrast, was selected to obtain particulate matter suspended in the waters of the longest and largest river in Norway that drains an area also with seasonal snow cover and high precipitation levels. The third site considered provided settling particulate matter from a trap in a lake from a mid-mountain catchment with a Mediterranean vegetation cover, which is only occasionally snow covered a few days a year. As I-brGDGTs were expected to reflect contributions from living biomass at the time of sampling (Weijers et al., 2011), we also analyzed the occurrence of I-brGDGTs from samples in two of the river catchments (Ulldeter and Øsaker).

# 2. Study sites and methods

## 2.1. Sample collection

### 2.1.1. NE Iberian Peninsula

One set of samples was collected in the Lake Montcortés catchment (42°19'50’’ N, 0°59'41’’ E, 1,027 m a.s.l.), located in the southern Catalan pre-Pyrenees (Fig. 1c). The catchment lies on a karstic terrain composed of Triassic materials (Rosell, 1994). There is no meteorological station in Lake Montcortés. Consequently, meteorological data were obtained from a nearby station located in the town of La Pobla de Segur (585 m a.s.l.), which is about 10 km from the study area. To take into account the higher elevation of Montcortés Lake, we estimated the rate of temperature change with altitude in the study region as 1 °C per 100 m in elevation. This was calculated using air temperature data from three meteorological stations near Montcortés in the towns of Sort, El Pont de Suert and La Pobla de Segur from September 2013 to May 2015. The annual mean air temperature (MAT) was estimated to be 8.5 °C, ranging from -3.3 °C in January to 17.6 °C in July during the sampling period at the elevation of Montcortés. For the period 1961-1990, the average accumulated annual precipitation in Pobla de Segur was 669 mm, with February as the driest month (33 mm) and May as the wettest month (88 mm). However, during the sampling year (2014), the precipitation was more variable, with March as the driest month (25 mm) and August as the wettest (155 mm) (Fig. 2a). The catchment is covered by evergreen/deciduous oak forests, conifers, grasses and littoral vegetation (Rull and Vegas-Vilarrúbia, 2015). From September 2013 to November 2014, soil samples (Ms1, Ms2 and Ms3) were obtained monthly from three different sites with different vegetation cover. For each soil type, three replicates (at least 5 m apart from each other within a 10 m radius area) were collected from an area of 400 $cm^2$ and a depth of 5 cm, after removing leaf litter and clearing the surface from any visible traces of vegetation. The soils were placed in a pre-combusted aluminium tray, wrapped with aluminium foil and sealed in plastic bags. Settling particles were collected in Montcortés Lake using a PVC tube, capped at one end, with a diameter of 8.5 cm and deployed at 20 m depth. Every month the trap was retrieved, and its contents were filtered through Whatman glass fibre filters (GF/F, 0.7 µm pore diameter). Samples were frozen on arrival at the laboratory until analysis.

A second series of measurements was undertaken in samples from Ulldeter, a glacial cirque in the Catalan Pyrenees (Fig. 1c), and the headwaters of the Ter river. From June 2010 to May 2011, the MAT (from a local meteorological station at 42°25' N, 2°15' E, 2364 m a.s.l.) in Ulldeter was 3.3 °C, ranging from -2.8 °C in January to 12.7 °C in July. The accumulated annual precipitation was 1264 mm, with October as the wettest month (228 mm) and February as the driest month (44 mm) (Fig. 3a). The area was covered with snow from November to March. The temperature and precipitation data in Ulldeter (Servei Meteorològic de Catalunya, 2011) during the studied periods are shown in Fig. 3. Soil samples were collected in a flat terrain, 100 m northwards from the meteorological station. Three soil replicates were taken each time, at least 5 m apart from each other within a 10 m radius area. The first 3 cm, corresponding to plant litter, were removed and the 2 cm of topsoil was sampled from a surface area of 100 $cm^2$. Samples were stored in plastic bags and frozen at -20 °C on arrival at the laboratory until analysis. The source of Ter River is close to the sampling site. In spring and summer 2011 two sediment traps were installed for a month: one was in an ephemeral stream that fed the Ter River (Trap A, 2300 m a.s.l.) running down from a mountain slope, the other was deployed in a small meander in the Ter River (Trap B, 2274 m a.s.l., attached to the stream bed). The trap contents were filtered through Whatman glass fibre filters (GF/F, 0.7 µm pore diameter) and stored frozen at -20 °C until analysis.

### 2.1.2. Southern Norway

Samples were collected near Øsaker, in a research farm located in the municipality of Sarpsborg situated 300 m away from Lake Vestvannet, which drains into the Glomma River (Fig. 1b). The meteorological station is located at the sampling site (59°19' N, 11°02' E, 45 m a.s.l.). During the sampling year (December 2010 – November 2011), MAT was 6.0 °C, ranging from -10.9 °C in December to 17.1 °C in July (Fig. 4a). The soil temperature at 10 cm depth showed a similar variability to air temperature in Øsaker, but the average annual soil temperature (7.7 °C) was 1.7 °C higher than local MAT. The accumulated annual precipitation was 1033 mm, with September (236 mm) as the wettest month and December (20 mm) as the driest month (NIBIO Agro MetBase, http://lmt.bioforsk.no). Each month soils were sampled in a forested area, 70 m away from the meteorological station. The top, corresponding to plant litter, was removed using a pick and a shovel. The first 2 cm of topsoil were sampled from an area of 100 $cm^2$. The sampling site for the water collection is located 6 km southeast of the meteorological station and 16 km upstream from the Glomma River mouth to the Skagerrak. Water samples (10 L of water) were collected from the Glomma River 0.5 m under the surface at Sandesund (Sarpsborg; 59°16' N, 11°05' E, 2.5 m a.s.l.) each month from February 2011 to January 2012. Water samples were sequentially filtered through Whatman glass fibre filters (GF/F, 0.7 µm pore diameter) for GDGT analysis. Samples were frozen on arrival at the laboratory.

## 2.2. Sample preparation

Montcortés soils (2-8 g, dry weight) were extracted with a mixture of 30 mL of dichloromethane:methanol (DCM:MeOH, 3:1, v/v, ×3) using a CEM-MARS microwave extractor (Kornilova and Rosell-Melé, 2003). After cooling to room temperature, the total extract was evaporated to near dryness and then fractionated over an aminopropyl silica column with 12 mL DCM:isopropanol (2:1, v/v; F1) and 15 mL diethyl ether:acetic acid (96:4, v/v; F2). Fraction F1 was then eluted through a silica column using hexane (6 mL, *n*-alkanes), DCM (4 mL, alkenone) and DCM:MeOH (95:5, v/v, 6 mL, GDGTs). The fraction containing GDGTs was dried with a vacuum centrifugal concentrator, re-dissolved with hexane:isopropanol (99:1, v/v), and filtered before instrumental analysis.

Filters from sediment traps of the Montcortés lake were extracted in a sonication bath with 20 mL of DCM:MeOH (3:1,v/v, x3), and centrifuged. Supernatants from the same sample were combined and dried by rotary evaporation. The extract was fractionated with 0.6 g silica (230-400 mesh; deactivated with 1% $H_2O$) using hexane (5 mL), DCM (4 mL), DCM:MeOH (95:5, v/v; 6 mL; GDGT fraction) and MeOH (5 mL). The GDGT fraction was fractionated further through an aminopropyl-silica (0.8 g; 4 0-60 µm particle size) column using DCM:isopropanol (2:1, v/v; 8 mL). The extract was dried and filtered through a 0.45 µm PTFE filter prior to instrumental analysis

Soil and river water samples from Ulldeter and Øsaker were prepared according to the procedure described by Huguet et al. (2010b). The samples were extracted in an ultrasonic bath using MeOH (×3), DCM:MeOH (1:1, v/v; ×3) and finally DCM (×3). After each sonication, samples were centrifuged and all the supernatants were combined, and taken to dryness using a vacuum centrifugal concentrator. The lipid extracts were fractionated with 0.5 g of activated silica and eluted with hexane:DCM (9:1, v/v; 3 mL; F1), hexane:DCM (1:1, v/v; 3 mL; F2) and DCM:MeOH (1:1, v/v; 3 mL; F3; GDGTs). The last fraction containing both core GDGTs (C-GDGT) and intact polar GDGTs (I-GDGT) was divided into two parts. One part was filtered through a 0.45 µm PTFE filter and stored until instrumental analysis. The other half was hydrolyzed to remove the polar head groups and to allow quantification of both core and intact polar lipids (Huguet et al., 2010b). Hydrolysis was performed with 2 mL of 5% HCl in MeOH (v/v) at 70 °C for 4 h. GDGTs were recovered by a liquid-liquid extraction using DCM and deionized water (1:1, v/v).The recovered DCM extracts were combined and rinsed six times with deionized water to remove any traces of HCl. The extracts were dried and filtered through a 0.45 µm PTFE filter prior to instrumental analysis.

## 2.3. Instrumental analysis

GDGTs in Montcortés samples were analyzed by injecting 5-20 µL aliquots of the fractionated extracts in a high performance liquid chromatograph (HPLC; Agilent 1200 RRLC) Time-of-Flight (TOF) mass spectrometer (MicroTOF-Q, Bruker Daltonics) with an atmospheric pressure chemical ionization (APCI) interface set in a positive mode. GDGTs in Ulldeter and Øsaker samples were automatically injected in a Dionex P680 HPLC coupled to a Thermo Finnigan TSQ Quantum Discovery Max quadrupole mass spectrometer. Following the methods (Escala et al., 2007; Huguet et al., 2013c), the extracts were eluted through a Tracer Excel CN column (Teknokroma; 20 cm length, 0.4 cm diameter and 3 µm particle size) equipped with a pre-column filter and a guard column. The mobile phase was eluted with hexane:*n*-propanol (98.5:1.5, v/v) at a flow of 0.6 mL/min and the parameters of the APCI interface were set as follows to generate positive ion spectra: corona discharge 3 µA, vaporizer temperature 400 °C, sheath gas pressure 49 mTorr, auxiliary gas ($N_2$) pressure 5 mTorr and capillary temperature 200 °C. GDGTs were detected in selected ion monitoring (SIM) mode at (Schouten et al., 2007): m/z 1050, 1048, 1046, 1036, 1034, 1032, 1022, 1020, 1018 and 1208 (abbreviated as GR, which was used as the internal standard). Prior to extraction, GR standard that is a synthetic tetraether lipid with a structure typical of neutral archaeal membrane lipids (Réthore et al. 2007) was added to the sample. The reproducibility of the quantification of GDGTs using GR as a standard is higher than 90% (Escala et al., 2009).

## 2.4. Ancillary measurements

### 2.4.1. Water content and LOI

The total amount of organic carbon (TOC) in soil samples was estimated using the loss on ignition (LOI) method (Schumacher, 2002). Aluminium trays were combusted at 450 °C for 8 h. About 1 g of newly collected soil sample (in triplicate) was weighed (WW) in a combusted aluminium tray and dried (18 h) at 105 °C in the oven. The dried samples were weighed ($DW_{105}$) and heated at 550 °C in the muffle furnace for 4 h and left to cool down to room temperature before weighing them ($DW_{550}$). The LOI value was calculated using the equation as follows (Heiri et al., 2001):

$$\text{Water content (\%)} = (WW - DW_{105})/WW \times 100\%$$

$$\text{LOI (\%)} = (DW_{105} - DW_{550})/DW_{105} \times 100\%$$

The TOC was calculated according to generally accepted TOC/LOI ratio of 0.58 (De Vos et al., 2005):

$$\text{TOC (\%)} = 0.58 \times \text{LOI} \times 100\%$$

### 2.4.2. pH analysis

The freeze-dried soils were homogenized and sieved (2 mm mesh size) to remove roots and small stones. The pH of the soil was potentiometrically measured in a supernatant suspension of a 1 to 2.5 soil: water mixture (Thomas, 2000). About 10 g of sieved soil was placed into a wide-mouth polythene container and mixed with deionized water (25 mL). The container was capped and shaken 1 h with a reciprocating shaking machine. A pH meter (GLP22, Crison Instrument) with a glass-calomel combination electrode was calibrated with a buffer solution at pH 4.0 and 7.0. The samples were shaken for about 5 seconds and the sensing electrode was immersed inside to record the value when it was stabilized (1σ, 0.1 pH unit).

# 3. Results

## 3.1. Sites characteristics

The three sites showed clear differences and a marked interannual variability, in air temperature and rainfall during the sampling period (Figs. 2a, 3a, 4a). Specifically, there was a marked difference in the temperature range between the coldest and hottest month, with the amplitude of the range larger in Øsaker (28.0 °C) and Montcortés (20.9 °C) than in Ulldeter (15.5 °C). The mean annual rainfall was the highest in Ulldeter (1264 mm), followed by Øsaker (1034 mm) and Montcortés (793 mm) (Fig. 2a, 3a, 4a). The difference between the wettest and driest month was 184 mm, 215 mm and 136 mm, respectively.

The soil TOC varied substantially between the three sites. The lowest TOC contents were found in the two sites in the Pyrenees, ranging from 6.4 to 17.7 % (mean 11.6 ± 1.0 %) in Montcortés and from 7.6 to 34.3 % (mean 20.3±7.7%) in Ulldeter (Table 2,3). In contrast, the TOC values were more than twice as high, and fluctuated from 37.8 to 53.6 % (mean 49.3±4.1%) in Øsaker (Table 1). These results were in line with the spatial distribution of TOC in Europe, with much higher values of organic carbon in Scandinavia than in Southern European topsoils (Jones et al., 2004; De Brogniez et al., 2015). During a year, the TOC content of soils in Montcortés and Øsaker fluctuated in a range of 6.8% and 15.8%, respectively. Ulldeter soils showed larger ranges, with the highest TOC in February/March and the lowest in May (Supplementary material Table S3). TOC in soils was negatively correlated with air temperature ($R^2$=0.71, p<0.01), and positively correlated ($R^2$=0.96, p<0.01) with monthly accumulated amount of rainfall (<150 mm/month).

The soils from Montcortés, which had the lowest TOC values, were also the least acidic, with pH values that ranged from 7.0 to 7.9 (mean 7.3±0.5), typical of calcareous forest soils. Conversely, the soils with the highest TOC had the lowest pH values, from 4.8 to 6.8 (mean 5.5±0.6) in Ulldeter, and in Øsaker with values between 3.9 and 4.5 (mean 4.1±0.1), typical of cool-temperate humid deciduous or mixed deciduous and coniferous forest soils (Supplementary material Tables S2-4) (Sumner, 1999). The dominant soil types in three sites were Halciustoll (Ulldeter), Torriorthent (Montcortés, Ms3), and

Podzolicsoil (Øsaker) according to the soil classification system published by Sumner (1999). It is apparent that the seasonal variability of soil pH values in these three sites was very small.

## 3.2. brGDGT concentration and distribution in soils

Concentrations of C-brGDGTs (normalized to TOC) varied along the sampling period within the same orders of magnitude in the three sites, albeit higher average values occurred in Øsaker. In the Montcortés catchment they ranged from 5.5 to 21.8 μg/g $_{TOC}$ (mean 11.4±4.9 μg/g $_{TOC}$), from 2.3 to 20.1 μg/g $_{TOC}$ (mean 10.9±4.7 μg/g $_{TOC}$) in Ulldeter soils, and from 3.3 to 73.2 μg/g $_{TOC}$ (mean 27.5±24.8 μg/g $_{TOC}$) in Øsaker soils (Fig. 2b, 3b, 4b). Previous studies reported that soils showed concentrations of C-brGDGTs from 1.2 to 10.9 μg/g $_{TOC}$ in soils from the Lake Challa catchment in east Africa (Buckles et al., 2014), from 1.3 to 17.5 μg/g $_{TOC}$ in the Iberian Peninsula (Menges et al., 2014) and from 0 to 12 μg/g $_{TOC}$ in Chinese soils (Yang et al., 2014a). In addition, all the C-brGDGT concentrations are in the range of mid-latitude soils without seasonal variation (Weijers et al., 2011).

The I-brGDGT (not analyzed in Montcortés) concentrations were also within the same order of magnitude in the two sites, but higher in Øsaker on average. In Ulldeter, the I-brGDGT abundance showed similar values (4.8-24.4 μg/g $_{TOC}$, mean 9.7±6.9 μg/g $_{TOC}$) to C-brGDGT from December to May, and lower values (<2.8 μg/g $_{TOC}$, mean 1.3±0.9 μg/g $_{TOC}$) than C-brGDGT (>5.0 μg/g $_{TOC}$) from June to November (Fig. 3b). In Øsaker the soil I-brGDGT concentrations were similar to C-brGDGT concentrations, ranging between 0.6 and 56.2 μg/g $_{TOC}$ with a mean value of 20.2±20.1 μg/g $_{TOC}$, showing higher concentrations from March to June. Our data seem to contrast with those of previous studies which reported that I-brGDGTs comprised only a smaller part of the total pool of branched GDGTs (e.g. Weijers et al., 2009; Peterse et al., 2010), as both pools of lipids have similar range of values in our samples. Our data do not seem to support the notion that production of brGDGTs from the living biomass is warm-season biased (e.g. Deng et al., 2016). In contrast, the highest concentration of I-brGDGTs in Ulldeter soils in December indicated a signature towards cold temperatures. In comparison with Ulldeter soils and soils from other sites where C-brGDGTs are dominant (Weijers et al., 2009, 2011; Huguet et al., 2010b; Tierney et al., 2012), the concentrations of I-brGDGTs in Øsaker soils varied within a larger range of values.

The distributions of C-brGDGTs and I-brGDGTs were nearly homogenous over time in the soils from the same site, but were dissimilar among the different sampling sites (Fig. S2). The dominant brGDGTs (Supplementary material Fig. S1) in Montcortés soils for sites Ms1, Ms2 and Ms3 were IIa, IIIa and IIb (>70%), followed by Ia, Ib. BrGDGT-IIa, Ia and IIIa were generally the most abundant compounds (55-84%) in Ulldeter soils, followed by IIb, Ib. BrGDGT-Ia and IIa were the most abundant ones (>90%) in Øsaker soils, followed by IIIa. The average distribution pattern in Montcortés and Ulldeter soils is similar to those in Tagus river catchment (Zell et al., 2014b) and in Øsaker soils is similar to that of soils from the Svalbard archipelago in the Arctic area reported by Weijers et al. (2007). The distribution/relative abundance of each compound in the same soil did not change much over the sampling year (Supplementary material Tables S2-4), as it will be discussed when analyzing the variability of the brGDGT ratios.

## 3.3. brGDGT fluxes and distributions in particulate matter

In Montcortés Lake, the aim was to monitor the C-brGDGT variations every month in vertical settling flux of particulate matter. The lowest fluxes occurred from January to June, and the highest fluxes from July to December (Fig. 2a), varying from 0.59 (μg/m$^2$/day) in February/March to about 8.45 (μg/m$^2$/day) in September/December. The observed trend in the annual cycle of the fluxes in Montcortés resembles those described for the temperate lakes Lower King Pond in Vermont (USA) (Loomis et al., 2014) and lake Lucerne in Switzerland (Blaga et al., 2011), and two tropical lakes (Challa and Huguangyan Maar) (Buckles et al., 2014; Hu et al., 2016). The magnitudes of the ranges in the C-brGDGT fluxes were also within the same order of magnitude in the 5 different lakes, being 0.1-20.0 μg/m$^2$/day in the Lower King Pond, between 0.84-3.0 ng/m$^2$/day (42 m) and 0.87-11.7 ng/m$^2$/day (72 m) in lake Lucerne; 0-12.0 μg/m$^2$/day in the Challa lake, and 3.2-24.2 μg/m$^2$/day in the Huguangyan Maar lake.

In Ulldeter, the aim was to collect recently eroded soil particulate matter, carried by runoff from snowmelt and after episodes of rainfall. Given that the ground was frozen and covered with snow for 5 months, the sampling was only undertaken during spring and summer, when ephemeral streams appeared in the mountainside below the soil sampling site. The accumulated abundance of C- and I-brGDGTs in spring (0.60 and 0.34 µg/g dry weight) was higher than in summer (0.26 and 0.15 µg/g dry weight), which might be due to co-effects of snowmelt and precipitation in spring (Fig. 3a).

In Øsaker, given the proximity of the Glomma River to the soil sampling site, the particulate matter derived from the runoff was obtained from the filtration of water samples in this river. The samples containing C-brGDGTs during the study period varied in concentration from 1.6 ng/L in February to 54.3 ng/L in April. The abundance of I-brGDGTs was much lower than C-brGDGTs in Glomma River, ranging between 0.2-3.0 ng/L in 9 out of the 12 samples, similar to the distribution of these brGDGTs (I-brGDGTs and C-brGDGTs) in Columbia River (French et al., 2015). The highest I-brGDGT concentrations were found in March and December (above 21.9 ng/L; Fig. 5d). Both maxima in concentrations of C- and I-brGDGTs were offset by 1-2 months with the mean river discharge, that peaked from May to July in Glomma River at Solbergfoss (50 km north from Sandesund, where the samples were collected) during the period 1901–2007 (Global Runoff Data Centre, 2011) (Fig. 5d).

The Montcortés trap, during the sampling period, had a similar distribution of brGDGTs, on average, to the soils studied (Supplementary material Fig. S2, Table 2). BrGDGT-IIa and IIIa were the most abundant homologues (59-67 %) followed by brGDGT-Ia, IIb and Ib, and traces of IIb, IIc, and Ic, throughout the sampling period.

In the Ulldeter traps, the brGDGTs distributions were also relatively similar to those in soils, where brGDGT-IIa was generally the most abundant compound in the SPM, followed by Ia, and IIIa, and at lower abundance IIb and Ib (Supplementary material Fig. S2). However, the fractional abundance of brGDGT-IIIa increased by >5% on average in the traps compared with soils, while in the intact polar fraction, brGDGT-IIIa increased by more than 10% in trap B, deployed in Ter River.

In the Glomma River, the differences in the composition of brGDGTs in soils and SPM were significant. Thus, in both core and intact polar fraction, the IIa was the most abundant compound instead of the most abundant Ia in soils. In addition, the fractional abundance of IIIa increased by 5-10 times compared with that of soils, while the proportion of IIa and IIb only slightly increased. In contrast, the proportion of Ia was reduced to a half, and brGDGT-Ib, Ic and IIc were still present in smaller amount in both soils and the SPM (Fig. S2).

The distributions of C- and I-brGDGTs in Glomma SPM are similar to that of I-brGDGT in Yenisei river gulf and mouth SPM that showed decreased Ia and increased IIIa (De Jonge et al., 2015).

## 3.4. GDGT proxy ratios

The ratios measured derived from brGDGTs were the following:

MBT = [Ia+Ib+Ic]/[Ia+Ib+Ic+IIa+IIb+IIc+IIIa+IIIb+IIIc] (Weijers et al., 2007) (eq.1)

MBT' = [Ia+Ib+Ic]/[Ia+Ib+Ic+IIa+IIb+IIc+IIIa] (Peterse et al. 2012) (eq.2)

CBT = -Log[(Ib+IIb)/(Ia+IIa)] = 3.33-0.38×pH (n=114; $R^2=0.7$) (Weijers et al., 2007) (eq.3)

The C-brGDGT CBT and MBT soil values from the three sites were within the range of values in global soil compilations, although they are substantially different among each other. Thus, the values from our three sites span almost the whole range of reported CBT values so far and half the range of MBT values (Figs. 6a and 6b).

In Montcortés, the CBT values of C-brGDGTs (C-CBT values) in soils ranged from 0.19 to 0.50, and in settling particulate from 0.34 to 0.52, a similar range to the values in the soils in the catchment (Fig. 2). In Ulldeter soils, the C-CBT values varied over a wider range of values, from 0.52 to 1.54, which encompasses the values in the trap A of 0.84/0.83 (spring/summer), and in the trap B of 1.03/0.99 (spring/summer) (Supplementary material Table S3). The CBT values of I-brGDGTs (I-CBT values) ranged from 0.56 to 1.53 in Ulldeter soils and were highly correlated to C-CBT values ($R^2=0.85$, $p<0.01$). In the traps from Ulldeter the spring/summer I-CBT values were 0.77/0.78 (spring/summer) in the trap A and 0.99/0.98 (spring/summer) in the trap B, which are within the range of the soil values. In Øsaker soils, C-CBT values varied from 1.40 to 1.69 (with one extreme value of 0.77 in March), and from 0.83 to 1.68 in Glomma River SPM. The range of I-CBT values was from 1.16 to 1.66 in Øsaker soil, and from 0.93 to 1.35 in Glomma River SPM.

The MBT values ranged from 0.20 to 0.35 in Montcortés soils, from 0.25-0.42 in Ulldeter soils and from 0.49-0.62 in Øsaker soils. MBT from C-brGDGTs ranged from 0.21 to 0.26 in Montcortés traps that showed low values from April to July and higher values from August to March. MBT from brGDGT core lipids were 0.32/0.25 and 0.27/0.27 in Ulldeter Trap A and Trap B, in spring and summer, respectively, while MBT from I-brGDGTs were 0.31/0.32 and 0.24/0.24. MBT from brGDGT core lipids and intact polar lipids were within the range of 0.29-0.37 in Glomma River SPM over a year except for C-MBT in November and I-MBT in February that showed higher values around 0.60.

# 4. Discussion

## 4.1. Controls on brGDGT abundance

No significant correlations were observed between total brGDGT concentrations in the soils from the three sites and MAT, MAP (mean annual precipitation) or pH, indicating that no single factor was responsible for the brGDGT abundances in our samples. However, specific regional conditions may sometimes play a significant role in brGDGT occurrences. For example, under the same local regime of precipitation and temperature, the brGDGT concentrations in soils (normalized to TOC) varied by an order of magnitude, even in a small catchment such as the ones in Montcortés lake. Such variability suggests that precipitation and temperature do not directly influence brGDGT production in soils. However, the brGDGT abundance seemed to be somewhat related to soil water content in Montcortés soils ($R^2=0.43$, $p<0.05$, Fig. 7a). This correlation improved when we expanded the number of soil locations investigated in the catchment and used the average annual values of brGDGT concentration (when available) ($R^2=0.87$, $p<0.05$, Fig. 7b). This finding is consistent with that observed in many regions that the concentrations of brGDGTs correlate positively (strongly or moderately) with soil water content, and that humid soils may provide a more favourable environment for brGDGT production than drier soils, under the same climatic regime (e.g. Dirghangi et al., 2013; Yang et al., 2014a; Ding et al., 2015; Wang et al., 2017b). Other studies also showed that soil water content had a clear impact on the absolute concentrations of all brGDGTs, with higher abundance in wetter soils (e.g. Dang et al., 2016). This is also assumed to explain the result that the higher brGDGT abundance occurs mostly in Øsaker soils, which are more humid than the other two sites even though we did not analyze the soil water content in Ulldeter and Øsaker soils.

The brGDGT abundance/flux of particulate matter in the river/lake showed distinctive seasonal variations due to different transport drivers (Fig. 5). In Montcortés, the drivers of the brGDGT flux during the annual cycle were likely to be wind and precipitation. The former mode of transport, carrying soil particles to the lake, is operational throughout the year although likely to be more intense in summer (Supplementary material Table S2, Fig. 5b). In contrast, rainfall runoff will drive sediment input to the lake most significantly when there is a rainstorm (Corella et al., 2016). The brGDGT flux peak in December might be due to water column mixing (Fig.5b) (Trapote et al., 2018), as reported in other temperate and tropical lakes (e.g. Buckles et al., 2014; Hu et al., 2016). During the partial lake turnover, 'fossil' brGDGTs from a pool suspended and preserved in the lower water column might be resuspended and trapped, increasing the brGDGT flux in the trap. Conversely, in Ulldeter, spring snowmelt runoff was also likely to carry soil matter to the local streams, as well as precipitation in summer. Arguably these would be the periods with the highest loads of brGDGT in soil-eroded matter and settling particulate matter in the Ter River. In the Glomma River, the brGDGT abundance reached a maximum one month (April) before the highest discharge (May) that was driven by snowmelt and precipitation (Fig. 4a, 5c). The brGDGT abundance in the river seemed not to be directly related to mean monthly river discharge (Fig. 5d). Our data suggest that the observed variation in SPM in the Glomma River should result from a mixing of soil-derived and *in situ* produced brGDGTs, leading to the highest flux of brGDGT supply from the riverine in *situ* produced brGDGTs.

## 4.2. Regional environmental controls on brGDGT proxies

The mean values of the CBT-brGDGT index in our study and their correlation with soil pH values fits well with the trends previously observed from the compilation of global soil data (Fig. 6, e.g. Weijers et al., 2007). Thus, CBT is mainly controlled by pH on large spatial scales (regional or global scale; $R^2$=0.72, p<0.01), but the trends were not so significant at small scales (Fig. 6a). In contrast, the correlation between MBT values and pH is not so significant on a global scale ($R^2$=0.46; Fig. 6b).

However, if a subset of data is considered, using data from previously reported Iberian soils (Menges et al., 2014) and those from this study, a significant correlation of MBT with pH is also apparent ($R^2$=0.77, p<0.01) (Fig. 6b). A significant positive correlation between MBT' and soil water content has been reported previously, based on C6-methylated brGDGTs (e.g. Dang et al., 2016; Naafs et al., 2017b). Instead, Naafs et al. (2017b) have established new global calibrations for temperature based on the finding that temperature is the primary control on C5-methyl brGDGTs in soils. Chromatographic separation and quantification of the C5- and C6-methylate isomers have improved the error statistics of temperature and pH calibrations based on brGDGTs in soils through the removal of the interference of the C6-methyl compounds from C5-methyl brGDGT fractional abundances (De Jonge et al., 2014b). Weber et al. (2015) analyzed sediment and watershed soils from a Swiss lake and documented the presence of a novel "mixed" hexa-methylated brGDGT that was only detected in the lake and not in soils of the surrounding watershed. This finding provided further evidence for *in situ* production of brGDGTs in lakes, increasing the possibility that separation of the 5- and 6-methyl isomers could be more useful. However, in our study, we did not separate C5 and C6-methylated brGDGTs, and the MBT' was generally higher in more humid soils (e.g. Ms1>Ms3).

Changes in soil pH and soil water content could explain a bias in the reconstructed MAT. The precise influence of different environmental factors on the estimation of MAT values is likely to be difficult to establish and will depend on local conditions in different sites or regions, or analytical improvements. For instance, in an extensive set of soils from humid, semi-humid to semi-arid and arid regions in China, the MBT/CBT derived temperatures matched the measured MATs better in humid and no-alkaline regions (Zheng et al., 2016). In our study, MAT was particularly underestimated in the estimates derived from the brGDGT indices in the more alkaline soils from Montcortés (Ms3) where pH values were higher. In contrast, values from the acidic Øsaker soils were overestimated (Fig. 8). It seems that soil water content and pH might constrain the suitability of brGDGT-proxies for continental air temperature reconstruction in some instances or locations, which affects the errors of any calibration. However, the overall global relationship is clearly strong. Thus, after the combination of our results with the data set published by Peterse et al. (2012) in Fig. S3, it is clear that the relationship between estimated and instrumental MAT is very close to a 1:1 line. As argued, any efforts to reduce the large errors in the

MBT/CBT-estimated MAT (Weijers et al., 2007; Peterse et al., 2012) should probably focus in regional calibrations efforts (e.g. Anderson et al., 2014; Yang et al., 2014b). Moreover, chromatographic separation of the 5-methyl and the 6-methyl isomers may improve the accuracy of the MAT estimates (De Jonge et al., 2014; Naafs et al., 2017).

## 4.3. Seasonality of the MAT estimates

Our data corroborate previous claims on the absence of seasonal patterns in the abundance and distribution of C-brGDGTs and I-brGDGTs in soils (e.g. Weijers et al., 2011). For instance, the reconstructed temperatures from C-brGDGTs (C-$MAT_{es}$ = 0.81-5.67×CBT+31×MBT´; Peterse et al. 2012) remained rather constant throughout the year in the Montcortés soils, and thus did not follow any climate seasonal variations (Fig. 8a). In the three sites of the catchment, C-$MAT_{est}$ values in soils ranged between 7.4-11.3 °C, 7.1-9.9 °C and 1.0-5.1 °C (Fig. 8a). In fact, some of the differences in the mean values of C-brGDGTs among the three Montcortés soils sites were larger than the annual variability within each site (Fig. 8a). Thus, the average C-$MAT_{est}$ reconstructed from samples Ms1 and Ms2 were 9.1±1.1 °C and 8.1±1.0 °C, respectively, equivalent to the instrumental MAT of 8.5 °C. While C-$MAT_{est}$ reconstructed from Ms3 was 3.1±1.0 °C, which was significantly colder than the instrumental MAT. This bias could be due to increased pH and aridity in Ms3, whose soils were located in a dry alkaline area. The lack of seasonality in the soil C-$MAT_{est}$ was also mirrored by the data from the settling particulate matter in Montcortés lake. The C-$MAT_{est}$ ranged between 4.1 and 6.8 °C, with an average of 5.1±0.7 °C, lying within the range of the three soil end members aforementioned. In fact, the annual variability in C-$MAT_{est}$ of the settling material in the lake is smaller than in soils. This phenomenon might be indicative that C-$MAT_{est}$ from materials in the sediment trap originated from the catchment soils, and that the C-$MAT_{est}$ in the lake sediments is mainly the weighted average from different soil inputs in the catchment.

The absence of a meaningful seasonal trend C-$MAT_{est}$ in soils from the Ulldeter site is also apparent, with values ranging between 0.1 and 7.8 °C (mean 3.6±2.2 °C) (Fig. 8b). At Ulldeter, the values of C-$MAT_{est}$ from the sediment Trap A (Fig. 8b), located at a higher elevation, also lacked a seasonal trend, with values higher in spring (6.0 °C) than summer (3.7 °C). These values were in fact closer to MAT (3.3 °C) than to real spring (2.3 °C) or summer temperature (10.2 °C). The C-MAT$_{est}$ for the sediments deposited in Trap B in the Ter River during spring and summer seasons were 3.4 °C and 3.5 °C, respectively (Fig. 8b), less variable than soil C-MAT$_{est}$ and also close to Ulldeter instrumental MAT (3.3 °C). The average value of the estimates from I-brGDGTs (i.e. I-MAT$_{est}$), which represents the inputs from living biomass at the sampling time, was 2.8 °C, 0.5 °C lower than instrumental MAT and 0.8 °C lower than soil C-MAT$_{est}$. The similarity of the C-MAT$_{est}$ data from both traps confirms the expectation that collected sediment resuspended in stream waters from the same source, which was eroded from original soils and the C-MAT$_{est}$ signal is representative of the overall standing stock of core lipids in soils.

Interestingly, the I-MAT$_{est}$ and C-MAT$_{est}$ values also showed a different variability pattern during the sampling period in the soils and in the traps (Fig. 8b), the variability being larger for I-MAT$_{est}$ than C-MAT$_{est}$. Such differences would endorse the proposal that these signals are derived from two different lipid pools, one associated to relic material (C-brGDGTs) and the other dominated by inputs from living biomass (I-brGDGTs). This was further supported by the few data that we obtained on I-brGDGTs from Trap A, where I-MAT$_{est}$ was 6.0 °C in June and increased to 10.5 °C in August, resembling the instrumental air temperatures rather than the signal from C-brGDGTs. The June I-MAT$_{est}$ was 0.8 °C lower than the instrumental June temperature, while the August I-MAT$_{est}$ was only 0.6 °C above the instrumental August temperature (11.1 °C). These data suggested that the distributions of I-brGDGTs in river particles may contain the new seasonal production signal from recently eroded soils or aquatic environments, which were not available from the measurement of C-brGDGTs. Thus, a seasonal bias in the MAT$_{est}$ would be obtained from the measurement of I-brGDGTs but not from C-brGDGTs in river particles, that would instead yield estimates closer to the actual MAT values. I-brGDGTs were under limit of quantification in Trap B from the Ter River samples.

In Øsaker soils, the C-MAT$_{est}$ ranged between 8.3 and 14.7 °C with an average of 10.7±1.5 °C, which is 4.7 °C above the instrumental MAT in Øsaker. Similarly, the I-MAT$_{est}$ ranged between 7.3 and 11.1 °C with an average of 9.5±1.2 °C (Fig. 8c). Consequently, there was no significant difference between C- or I-brGDGT based MAT estimates in soils. As in the other two sites, the amplitude of the seasonal cycle in the MAT in Øsaker was not reflected in the variability of the soil brGDGT MAT signatures. These have similar range of variability annually in the three sites, of ±5.1 °C in Montcortés (average), ±6.4 °C in Øsaker, and ±7.7 °C in Ulldeter. In comparison, the instrumental MAT variability is ±20.9 °C in Montcortés, ±28.0 °C in Øsaker, and ±15.5 °C in Ulldeter (Supplementary material Table S2-4).

Nevertheless, in Øsaker, the annual C-MAT$_{est}$ is also substantially warmer than the instrumental MAT, while in Ulldeter and Montcortés the C-MAT$_{est}$ was close to the instrumental value. This 'warm' signal in Øsaker soils might be due to the decreased fractional abundance of C6-methyl brGDGTs as the 'cold' underestimated MAT was observed in arid soils with a large amount of C6-methyl brGDGTs (De Jonge et al., 2014b). The Glomma River is the longest and largest river in Norway, with a basin area of 42,000 km$^2$, which drains 13% of Norway's area. Its course has a change in elevation of 690 m. Consequently, the sediment particles sampled near its mouth, obviously, will have a much wider range of sources than the soils taken in the Øsaker station. In that sense, there was no reason to expect that the brGDGTs signatures in the SPM should have the same patterns to surrounding soils as described so far for Montcortés and Ulldeter. In fact, the variability of C- and I-MAT$_{est}$ in Glomma River SPM was larger than in the Øsaker soils (Fig. 8c). However, we observed the same lack of seasonal pattern in C-MAT$_{est}$ already described in the settling particles of Montcortés Lake or the runoff from Ulldeter, which was also apparent in the I-brGDGT signatures. Moreover, the average C- and I-MAT$_{est}$ in the Glomma River particulate material was 5.0/5.2 °C, just 1 °C below the instrumental MAT at Øsaker, and lower than soil C-MAT$_{est}$. Such differences were rather small and might be attributed to the sources of the particles further upstream than Øsaker, in locations at higher elevations and with a continental climate (Rueda et al., 2009). These data further supported the notion that the standing stock of core lipids in soils was much higher than any new annual brGDGT production over a seasonal cycle, and that the slow turnover time, on timescales of decades, of brGDGTs occurred in terrestrial environments (e.g. Weijers et al., 2010; Huguet et al., 2017). This may provide an explanation as to why the bulk of the soil brGDGT signature is in fact largely representative of average annual air temperatures, independently of the annual amplitude of the local temperature seasonal cycle. Consequently, the bulk of the eroded soil signal represented by the brGDGTs, being carried to river courses and eventually to a sedimentary environment, would not be seasonally biased and could be best used to estimate MAT in the regions investigated.

## 4.4. Particulate matter brGDGT sources

In the areas investigated in our study, we propose that the main sources of brGDGTs in the particulate matter are the soils from the lake or stream catchment. This interpretation is based on the observations that, i) the brGDGT distributions in soils and the particulate matter have more points of similarity than otherwise, and, ii) the lack of seasonality in the proxy signals in the three settings, both in the soils and particulate matter signals. The latter argument assumes that the turnover time of brGDGTs in particulate matter would be on seasonal time-scales rather than decades or centuries as reported for soils and peatlands (e.g. Weijers et al., 2010; Huguet et al., 2017).

However, this conclusion would appear to contradict the well-established notion in the literature that, in aquatic settings, brGDGTs are mainly derived from *in situ* sources, rather than allochthonous ones. This notion has been sustained, mainly, on the description of different brGDGT distributions in sediments in relation to those in soils on adjacent lands (e.g. Sinninghe Damsté et al., 2009, 2016; Bechtel et al., 2010; Loomis et al., 2011, 2014; Sun et al.,2011; Tierney et al., 2012; Schoon et al., 2013; Ajioka et al., 2014a; Buckles et al., 2014; Naeher et al., 2014; Colcord et al., 2015; Weber et al., 2015; Warden et al., 2016; Zink et al., 2016). In addition, some brGDGTs have only been identified in lacustrine sediments that had a distinct carbon isotopic signature from brGDGTs in soils (Weber et al., 2015). Fietz et al. (2012) also argued that the widespread significant correlation between concentrations of brGDGTs and crenarchaeol, a common archaeal biomarker in aquatic settings (e.g. Schouten et al., 2013), could be interpreted as evidence of *in situ* production of brGDGTs in lacustrine and marine settings. Moreover, the occurrence of the intact form of brGDGTs in living cells (I-brGDGT) across the continuum from soil to marine environments can also be construed as evidence for the widespread *in situ* production of brGDGTs in a wide range of environments (e.g. French et al., 2015).

However, some studies have also noted that in some instances the distributions of brGDGTs in a lake catchment soils and sediments are similar (e.g. Niemann et al., 2012; Hanna et al., 2016). Peterse et al.

(2015) observed no *in situ* production of brGDGTs, but did observe production of archaeal (i.e. isoprenoidal) GDGTs, in 160-day incubations of soils in fresh and ocean water. In the Colville, Congo and Danube river contributions from *in situ* derived brGDGTs were not deemed significant in relation to the signal derived from local soil inputs within the drainage basin and ultimately exported to the sea (Hanna et al., 2016; Freymond et al., 2017; Hemingway et al., 2017). In the Baltic Sea, significant *in situ* production was also deemed unlikely given the correlation between brGDGTs and terrigenous indicators (Kaiser and Arz, 2016). These findings and our study would show that, even though *in situ* production may be widespread, it is not necessarily always the dominant source of brGDGTs in all aquatic settings. Clearly, this poses an added difficulty in the choice of the most appropriate calibration in sedimentary palaeorecords (i.e. soil vs. sediments), which can be compounded if the relative inputs from allochthonous vs autochthonous sources change as well through time.

Regarding the lack of seasonality in the brGDGT proxies in the settling particulate matter, as already noted, this is not the first study to make such an observation. Loomis et al. (2014), in a small and relatively shallow kettle lake in northern Vermont argued that the lack of seasonality was caused by a dominance of inputs into the trap (at 6.5 m depth) from the lake subsurface rather than from surface production of brGDGTs, or from surrounding soils. In our study in the Montcortés trap, we do not have any evidence that significant *in situ* production of brGDGTs is occurring in the Montcortés lake. We propose that the simplest explanation is that the main source of brGDGTs is the lake catchment, from its soils. The non-seasonal signals in the soils are transferred into the settling particles in the trap, which have a distribution of brGDGTs that appear to be a weighted mean of the soil signals (Fig. 8a). It is not surprising that, even in a small catchment as in Lake Montocortés, the soils are spatially chemically heterogenous. By their very nature many soils are heterogenous even at small spatial scales (e.g. Jackson and Caldwell, 1993). How the different soils from a catchment may contribute to the settling particle signals may depend on, i) the facility with which each site erodes, ii) its location in the catchment so the soil particles via runoff reach the lake, and, iii) the concentrations of brGDGTs in each soil location, which is correlated to soil water content in the Montcortés catchment (Fig. 7). The relative importance of different areas of the catchment as a source of brGDGTs may change over time, through change in land uses and/or climatic/weather events (Corella et al., 2011, 2016).

Moreover, other potential sources that may deserve further investigation are the aeolian inputs into the lake. Dust is composed of soil and sediment particles that contains brGDGTs (e.g. Fietz et al., 2013), and can contribute significantly to the exported sedimentary signal to the deep sea (e.g. Yamamoto et al., 2016; Jaeschke et al., 2017). In continental settings, eolian inputs of brGDGTs have not been taken into consideration to explain sedimentary or loess/paleosols sequences except in a very few instances (e.g. Zech et al., 2012). Further research should focus on the degree to which atmospheric redeposition, by the eolian transport of GDGTs, might overprint local signals in a particular site.

# 5. Conclusions

No seasonal trends were observed in the distribution of brGDGTs in soils from environments with a large amplitude in the seasonal cycle of temperature and precipitation. Results confirmed previous findings from mid-latitude soils, on the lack of a detectable short-term seasonal signal on the background soil brGDGT distributions. Moreover, we show that the brGDGT signatures in particulate materials derived from the same catchment also lacked a seasonal pattern.

Conversely, the brGDGT production in different types of soils from different catchments varied during an annual cycle. The temporal variability of brGDGTs is not coupled to the annual cycle of temperature and precipitation, nor is transferred to the brGDGT proxy indices, i.e. CBT-MBT('). In fact, the dependence of these proxies with annual mean pH and air temperature is robust, particularly when analyzed at large spatial scales (i.e. continental). Moreover, this climatic signal is transferred to the sediments derived from runoff in the catchment as the particulate matter in the three environments had very similar $MAT_{est}$ values in soils.

The interpretation of the reconstruction of any proxy requires an understanding of the spatial and temporal scales on which the reconstructed parameters are representative of. In our study, we provide further evidence that the brGDGT signatures in depositional environments are representative of the soils in the hydrological catchment. In addition, we demonstrate that the sedimentary signal is unlikely to contain a seasonal bias when derived from soil sources. The accuracy of brGDGT-derived temperature estimates based on MBT/CBT proxy in soils will depend on soil properties rather than seasonal signals.

Furthermore, soils are likely to contain a brGDGT signature which is representative of average environmental conditions in the catchment over decades if not longer time scales, depending on the soil type and the age of the carbon stocks. Consequently, brGDGT proxy reconstructions based on soil and peat sources of brGDGTs should be considered to infer variability in environmental parameters over the same timescales (i.e. decades or longer). On shorter timescales (i.e. annual), sediment downcore variability is likely to be related to changes derived from *in situ* production and sediment sources.

## Acknowledgements

We thank N. Moraleda, F. Colomer, M. Raja for help with soil sampling, R. Gyllencreutz for facilitating the Norwegian field sampling, and J. M. Alcañiz for facilitating the soil pH analysis. Meteorological data in Pobla de Segur were provided by J. Sigró. This work was supported by Spanish Ministry of Research (projects TETRACLIM ref. CGL2010-15000 and Montcortés-500 ref. CGL-2012-33665), a Maria de Maeztu award MDM-2015-0552, a PhD studentship to G.R. from the Spanish Ministry of Science (FPU AP2008-00801), and a studentship 492 to M.C, from the China Scholarship Council (CSC). Many thanks to the anonymous reviewers who have provided constructive suggestions to improve the manuscript.

## Figures

**Figure 1.** a) General location of the study areas; b) Øsaker, southern Norway; c) Montcortés and Ulldeter, Catalan Eastern Pyrenees. Maps obtained from the software Ocean Data View (Schlitzer, 2010). The circles indicate the locations of sampling sites.

**Figure 2**. a) Monthly accumulated precipitation (bars) and instrumental monthly mean air temperature (lines) in Pobla de Segur (10 km from Lake Montcortés); b) Average concentrations of C-brGDGT (brGDGT core lipids) in the Lake Montcortés catchment and; c) Average brGDGT-derived CBT and MBT indices in Montcortés soils from September 2013 to November 2014. The error bars show the range for the values from three different soils in the catchment.

**Figure 3**. a) Monthly accumulated precipitation (bars) and instrumental monthly mean air temperature (lines) in Ulldeter; b) Concentrations of core (C-brGDGT) and intact polar (I-brGDGT) branched GDGTs in the Ulldeter soils and; c) C-brGDGT and I-brGDGT derived CBT and MBT indices in Ulldeter soils from June 2010 to May 2011.

**Figure 4**. a) Monthly accumulated precipitation (bars) and instrumental monthly mean air temperature (lines) in Øsaker; b) Concentrations of core (C-brGDGT) and intact polar (I-brGDGT) branched GDGTs in Øsaker soils; and c) C-and I-brGDGT derived CBT and MBT indices in Øsaker soils from December 2010 to November 2011.

**Figure 5**. a) Temperature and precipitation in Montcortés (Pobla de Segur); b) Flux of core branched GDGTs in the sediment trap in Lake Montcortés from October 2013 to November 2014. c) Temperature and precipitation in Øsaker; d) Concentration of brGDGTs in suspended particulate matter (SPM) from the Glomma River. Concentration of C-brGDGTs (hollow diamonds) and I-brGDGTs (crosses) are

compared to mean discharge ($m^3/s$, discontinous line) of Glomma River at Solbergfoss for the period 1901-2007 (Global Runoff Data Centre, 2011).

**Figure 6**. Linear regression plots of global data on (a) measured soil pH vs. CBT, and (b) measured soil pH vs. MBT indx data. Data plotted in black and blue are from Weijers et al. (2007) and Menges et al. (2014), respectively, data plotted in other colours are from this study.

**Figure 7**. The relationship between soil water content and core brGDGT concentration in Montcortés catchment: a) Values from the monthly sampling over the study period (September 2013-November 2014) from sites Ms1, Ms2 and Ms3, characterized by grassland, oak forest and upland dry grassland/scrubland, respectively. b) Values of 6 soil sites around the Montcortés lake, where Ms1, Ms2, Ms3 represent the average values during the study period, whereas sites Ms4, Ms5, Ms6 were only sampled once in January 2016.

**Figure 8.** Meteorological data and GDGT based temperature estimates for soils from Montcortés (a), Ulldeter (b) and Øsaker (c). Monthly instrumental mean temperature is given as MMAT (black continuous line with crosses) and average instrumental values during the study period as MAT (black dashed lines). The results for the GDGT based estimates (MBT'/CBT) based on core GDGTs (C-MATest, solid diamonds) and intact GDGTs (I-MATest, hollow diamonds) are shown for the monthly sampled soils. The results for the sediment traps (in Montcortés lake and Ulldeter streams) and water samples (in Glomma River) are shown with blue diamonds (C-MATest), and hollow blue diamonds (I-MATest).

## References

Ajioka, T., Yamamoto, M., Murase, J., 2014a. Branched and isoprenoid glycerol dialkyl glycerol tetraethers in soils and lake/river sediments in Lake Biwa basin and implications for MBT/CBT proxies. Organic Geochemistry 73, 70–82.

Ajioka, T., Yamamoto, M., Takemura, K., Hayashida, A., Kitagawa, H., 2014b. Water pH and temperature in Lake Biwa from MBT'/CBT indices during the last 280 000 years. Climate of the Past 10 (5), 1843–1855.

Anderson, V.J., Shanahan, T.M., Saylor, J.E., Horton, B.K., Mora, A.R., 2014. Sources of local and regional variability in the MBT'/CBT paleotemperature proxy: Insights from a modern elevation transect across the Eastern Cordillera of Colombia. Organic Geochemistry 69, 42–51.

Ayari, A., Yang, H., Wiesenberg, G.L.B., and Xie, S., 2013. Distribution of archaeal and bacterial tetraether membrane lipids in rhizosphere-root systems in soils and their implication for paleoclimate assessment. Geochemical Journal 47 (3), 337–347.

Ballantyne, A.P., Greenwood, D.R., Sinninghe Damste, J.S., Csank, A.Z., Eberle, J.J., Rybczynski, N., 2010. Significantly warmer Arctic surface temperatures during the Pliocene indicated by multiple independent proxies. Geology 38, 603–606.

Bechtel, A., Smittenberg, R.H., Bernasconi, S.M., Schubert, C.J., 2010. Distribution of branched and isoprenoid tetraether lipids in an oligotrophic and a eutrophic Swiss lake: Insights into sources and GDGT-based proxies. Organic Geochemistry 41, 822–832.

Bendle, J.A., Weijers, J.W.H., Maslin, M.A., Sinninghe Damsté, J.S., Schouten, S., Hopmans, E.C., Boot, C.S., Pancost, R.D., 2010. Major changes in glacial and Holocene terrestrial temperatures and sources of organic carbon recorded in the Amazon Fan by tetraether lipids. Geochemistry, Geophysics, Geosystems 11, 1–13.

Blaga, C.I., Reichart, G.J., Heiri, O., and Sinninghe Damsté, J.S., 2009. Tetraether membrane lipid distributions in water-column particulate matter and sediments: a study of 47 European lakes along a north–south transect. Journal of Paleolimnology 41(3), 523–540.

Blaga, C.I., Reichart, G.-J., Schouten, S., Lotter, A.F., Werne, J.P., Kosten, S., Mazzeo, N., Lacerot, G., Sinninghe Damsté, J.S., 2010. Branched glycerol dialkyl glycerol tetraethers in lake sediments: can they be used as temperature and pH proxies? Organic Geochemistry 41, 1225–1234.

Blaga, C.I., Reichart, G.J., Vissers, E.W., Lotter, A.F., Anselmetti, F.S., and Sinninghe Damsté, J.S., 2011. Seasonal changes in glycerol dialkyl glycerol tetraether concentrations and fluxes in a perialpine lake: Implications for the use of the $TEX_{86}$ and BIT proxies. Geochimica et Cosmochimica Acta 75(21), 6416–6428.

Blyth, A.J., Schouten, S., 2013. Calibrating the glycerol dialkyl glycerol tetraether temperature signal in speleothems. Geochimica et Cosmochimica Acta 109, 312–328.

Buckles, L.K., Weijers, J.W.H., Verschuren, D., Sinninghe Damsté, J.S., 2014. Sources of core and intact branched tetraether membrane lipids in the lacustrine environment: Anatomy of Lake Challa and its catchment, equatorial East Africa. Geochimica et Cosmochimica Acta 140, 106–126.

Cao, J., Rao, Z., Jia, G., Xu, Q., Chen, F., 2017. A 15 ka pH record from an alpine lake in north China derived from the cyclization ratio index of aquatic brGDGTs and its paleoclimatic significance. Organic Geochemistry 109, 31–46.

Coffinet, S., Huguet, A., Anquetil, C., Derenne, S., Pedentchouk, N., Bergonzini, L., Wagner, T., 2017. Evaluation of branched GDGTs and leaf wax n-alkane $\delta^2H$ as (paleo) environmental proxies in East Africa. Geochimica et Cosmochimica Acta 198, 182–193.

Colcord, D.E., Cadieux, S.B., Brassell, S.C., Castañeda, I.S., Pratt, L.M., White, J.R., 2015. Assessment of branched GDGTs as temperature proxies in sedimentary records from several small lakes in southwestern Greenland. Organic Geochemistry 82, 33–41.

Corella, J.P., Moreno, A., Morellon, M., Rull, V., Giralt, S., Rico, M.T., Valero-Garcés, B.L., 2011. Climate and human impact on a meromictic lake during the last 6,000 years (Montcortès Lake, Central Pyrenees, Spain). Journal of Paleolimnology 46(3), 351–367.

Corella, J.P., Valero-Garcés, B.L., Vicente-Serrano, S.M., Brauer, A., Benito, G., 2016. Three millennia of heavy rainfalls in Western Mediterranean: frequency, seasonality and atmospheric drivers. Scientific Reports 6 (April), 38206.

Dang, X., Yang, H., Naafs, B.D.A., Pancost, R.D., 2016. Direct evidence of moisture control on the methylation of branched glycerol dialkyl glycerol tetraethers in semi-arid and arid soils. Geochimica et Cosmochimica Acta 189, 24-36.

Davtian, N., Ménot, G., Bard, E., Poulenard, J., - Podwojewski, P., 2016. Consideration of soil types for the calibration of molecular proxies for soil pH and temperature using global soil datasets and Vietnamese soil profiles. Organic Geochemistry 101, 140–153.

De Brogniez, D., Ballabio, C., Stevens, A., Jones, R.J.A., Montanarella, L., van Wesemael, B., 2015. A map of the topsoil organic carbon content of Europe generated by a generalized additive model. European Journal of Soil Science 66(1), 121–134.

De Jonge, C., Stadnitskaia, A., Hopmans, E.C., Cherkashov, G., Fedotov, A., Sinninghe Damsté, J.S., 2014a. In situ produced branched glycerol dialkyl glycerol tetraethers in suspended particulate matter from the Yenisei River, Eastern Siberia. Geochimica et Cosmochimica Acta 125, 476–491.

De Jonge, C., Hopmans, E.C., Zell, C.I., Kim, J.H., Schouten, S., Sinninghe Damsté, J.S., 2014b. Occurrence and abundance of 6-methyl branched glycerol dialkyl glycerol tetraethers in soils: implications for palaeoclimate reconstruction. Geochimica et Cosmochimica Acta 141, 97–112.

De Jonge, C., Stadnitskaia, A., Hopmans, E.C., Cherkashov, G., Fedotov, A., Streletskaya, I.D., Vasiliev, A.A., Sinninghe Damstéa, J.S., 2015. Drastic changes in the distribution of branched tetraether lipids in suspended matter and sediments from the Yenisei River and Kara Sea (Siberia): Implications for the use of brGDGT-based proxies in coastal marine sediments. Geochimica et Cosmochimica Acta 165, 200–225.

De Vos, B., Vandecasteele, B., Deckers, J., Muys, B., 2005. Capability of loss-on-ignition as a predictor of total organic carbon in non-calcareous forest soils. Communications in Soil Science and Plant Analysis 36 (19-20), 2899–2921.

Deng, L., Jia, G., Jin, C., Li, S., 2016. Warm season bias of branched GDGT temperature estimates causes underestimation of altitudinal lapse rate. Organic Geochemistry 96, 11–17.

Ding, S., Xu, Y., Wang, Y., He, Y., Hou, J., Chen, L., He, J.S., 2015. Distributions of glycerol dialkyl glycerol tetraethers in surface soils of Qinghai-Tibetan Plateau: Implications of GDGT-based proxies in cold and dry regions. Biogeoscience Discussion 12, 481–513.

Dirghangi, S.S., Pagani, M., Hren, M.T., Tipple, B.J., 2013. Distribution of glycerol dialkyl glycerol tetraethers in soils from two environmental transects in the USA. Organic Geochemistry 59, 49–60.

Ernst, N., Peterse, F., Breitenbach, S.F.M., Syiemlieh, H.J., Eglinton, T.I., 2013. Biomarkers record environmental changes along an altitudinal transect in the wettest place on Earth. Organic Geochemistry 60, 93–99.

Escala, M., Rosell-Melé, A., Masqué, P., 2007. Rapid screening of glycerol dialkyl glycerol tetraethers in continental Eurasia samples using HPLC/APCI-ion trap mass spectrometry. Organic Geochemistry 38, 161–164.

Escala, M., Fietz, S., Rueda, G., Rosell-Melé, A., 2009. Analytical considerations for the use of the paleothermometer tetraether index 86 and the branched vs isoprenoid tetraether index regarding the choice of cleanup and instrumental conditions. Analytical Chemistry 81 (7), 2701–2707.

Fawcett, P.J., Werne, J.P., Anderson, R.S., Heikoop, J.M., Brown, E.T., Berke, M.A, Allen, C.D., 2011. Extended megadroughts in the southwestern United States during Pleistocene interglacials. Nature 470 (7335), 518–521.

Fietz, S., Huguet, C., Bendle, J., Escala, M., Gallacher, C., Herfort, L., Rosell-Melé, A., 2012. Co-variation of crenarchaeol and branched GDGTs in globally-distributed marine and freshwater sedimentary archives. Global and Planetary Change 92–93, 275–285.

Fietz, S., Prahl, F. G., Moraleda, N., Rosell-Melé, A., 2013. Eolian transport of glycerol dialkyl glycerol tetraethers (GDGTs) off northwest Africa. Organic Geochemistry 64, 112–118.

French, D.W., Huguet, C., Turich, C., Wakeham, S.G., Carlson, L.T., Ingalls, A.E., 2015. Spatial distributions of core and intact glycerol dialkyl glycerol tetraethers (GDGTs) in the Columbia River Basin and Willapa Bay, Washington: Insights into origin and implications for the BIT index. Organic Geochemistry 88, 91–112.

Freymond, C.V., Peterse, F., Fischer, L.V., Filip, F., Giosan, L., Eglinton, T.I., 2017. Branched GDGT signals in fluvial sediments of the Danube River basin: Method comparison and longitudinal evolution. Organic Geochemistry 103, 88–96.

Gao, L., Nie, J., Clemens, S., Liu, W., Sun, J., Zech, R., Huang, Y., 2012. The importance of solar insolation on the temperature variations for the past 110kyr on the Chinese Loess Plateau. Palaeogeography, Palaeoclimatology, Palaeoecology 317–318 (1), 128–133.

Global Runoff Data Centre, 2011. Long term mean monthly discharge and annual characteristics of GRDC station. Koblenz, Germany: Federal institute of hydrology.

Hanna, A.J.M., Shanahan, T.M., Allison, M.A., 2016. Distribution of branched GDGTs in surface sediments from the Colville River, Alaska: Implications for the MBT′/CBT paleothermometer in Arctic marine sediments. Journal of Geophysical Research: Biogeosciences 121(7), 1762–1780.

Heiri, O., Lotter, A.F., Lemcke, G., 2001. Loss on ignition as a method for estimating organic and carbonate content in sediments : reproducibility and comparability of results. Journal of Paleolimnology 25, 101–110.

Hemingway, J.D., Schefuß, E., Spencer, R.G.M., Dinga, B.J., Eglinton, T.I., McIntyre, C., Galy, V.V., 2017. Hydrologic controls on seasonal and inter-annual variability of Congo River particulate organic matter source and reservoir age. Chemical Geology 466, 454–465.

Hopmans, E.C., Weijers, J.W., Schefuß, E., Herfort, L., Sinninghe Damsté, J.S., Schouten, S., 2004. A novel proxy for terrestrial organic matter in sediments based on branched and isoprenoid tetraether lipids. Earth and Planetary Science Letter 224 (1-2), 107–116.

Hu, J., Zhou, H., Peng, P., Spiro, B., 2016. Seasonal variability in concentrations and fluxes of glycerol dialkyl glycerol tetraethers in Huguangyan Maar Lake, SE China: Implications for the applicability of the MBT-CBT paleotemperature proxy in lacustrine settings. Chemical Geology 420, 200–212.

Huguet, A., Fosse, C., Laggoun-Défarge, F., Toussaint, M.L., Derenne, S., 2010a. Occurrence and distribution of glycerol dialkyl glycerol tetraethers in a French peat bog. Organic Geochemistry 41(6), 559–572.

Huguet, A., Gocke, M., Derenne, S., Fosse, C., Wiesenberg, G.L.B., 2013a. Root-associated branched tetraether source microorganisms may reduce estimated paleotemperatures in subsoil. Chemical Geology 356, 1–10.

Huguet, A., Fosse, C., Laggoun-Défarge, F., Delarue, F., Derenne, S., 2013b. Effects of a short-term experimental microclimate warming on the abundance and distribution of branched GDGTs in a French peatland. Geochimica et Cosmochimica Acta 105, 294–315.

Huguet, A., Grossi, V., Belmahdi, I., Fosse, C., Derenne, S., 2015. Archaeal and bacterial tetraether lipids in tropical ponds with contrasting salinity (Guadeloupe, French West Indies): Implications for tetraether-based environmental proxies. Organic Geochemistry 83–84, 158–169.

Huguet, A., Meador, T.B., Laggoun-Défarge, F., Könneke, M., Wu, W., Derenne, S., Hinrichs, K.U., 2017. Production rates of bacterial tetraether lipids and fatty acids in peatland under varying oxygen concentrations. Geochimica et Cosmochimica Acta 203, 103–116.

Huguet, C., de Lange, G.J., Gustafsson, O., Middlelburg, J.J., Sinninghe Damsté, J.S., Schouten S., 2008. Selective preservation of soil organic matter in oxidized marine sediments (Madeira Abyssal Plain). Geochimica et Cosmochimica Acta 72, 6061–6068.

Huguet, C., Martens-Habbena, W., Urakawa, H., Stahl, D., Ingalls, A.E., 2010b. Comparison of extraction methods for quantitative analysis of core and intact polar glycerol dialkyl glycerol tetraethers (GDGTs) in environmental samples. Limnology and Oceanography: Methods 8, 127–145.

Huguet, C., Fietz, S., Rosell-Melé, A., 2013c. Global distribution patterns of hydroxy glycerol dialkyl glycerol tetraethers. Organic Geochemistry 57, 107–118.

Jackson, R.B., and Caldwell, M.M., 1993. Geostatistical Patterns of Soil Heterogeneity Around Individual Perennial Plants. Journal of Ecology 81(4), 683-692.

Jaeschke, A., Wengler, M., Hefter, J., Ronge, T.A., Geibert, W., Mollenhauer, G., Lamy, F., 2017. A biomarker perspective on dust, productivity, and sea surface temperature in the Pacific sector of the Southern Ocean. Geochimica et Cosmochimica Acta 204, 120–139.

Jones, R.J.A., Hiederer, R., Rusco, E., Loveland, P.J. Montanarella, L., 2004. Topsoil Organic Carbon Content in Europe (Version 1.2). Special Publication Ispra No 72, map in ISO B1 format, European Commission Joint Research Centre, Ispra, Italy.

Kaiser, J., Arz, H.W., 2016. Sources of sedimentary biomarkers and proxies with potential paleoenvironmental significance for the Baltic Sea. Continental Shelf Research 122, 102–119.

Kim, J.H., Zarzycka, B., Buscail, R., Bourrin, F., Palanque, A., Sinninghe Damsté, J.S., Bonnin, J., Schouten, S., 2009. Transport and depositional process of soil organic matter during wet and dry storms on the Tęt inner shelf (NW Mediterranean). Palaeogeography Palaeoclimatology Palaeoecology 273 (3), 228–238.

Kornilova, O., Rosell-Melé, A., 2003. Application of microwave-assisted extraction to the analysis of biomarker climate proxies in marine sediments. Organic Geochemistry 34(11), 1517–1523.

Lei, Y., Yang, H., Dang, X., Zhao, S., Xie, S., 2016. Absence of a significant bias towards summer temperature in branched tetraether-based paleothermometer at two soil sites with contrasting temperature seasonality. Organic Geochemistry 94, 83-94.

Liu, W., Wang, H., Zhang, C.L., Liu, Z., He, Y., 2013. Distribution of glycerol dialkyl glycerol tetraether lipids along an altitudinal transect on Mt. Xiangpi, NE Qinghai-Tibetan Plateau, China. Organic Geochemistry 57, 76–83.

Liu, X.L., Zhu, C., Wakeham, S.G., Hinrichs, K.U., 2014. In situ production of branched glycerol dialkyl glycerol tetraethers in anoxic marine water columns. Marine Chemistry 166, 1–8.

Loomis, S.E., Russell, J.M., Sinninghe Damsté, J.S., 2011. Distributions of branched GDGTs in soils and lake sediments from western Uganda: Implications for a lacustrine paleothermometer. Organic Geochemistry 42(7), 739–751.

Loomis, S.E., Russell, J.M., Ladd, B., Street-Perrott, F.A., Sinninghe Damsté, J.S., 2012. Calibration and application of the branched GDGT temperature proxy on East African lake sediments. Earth and Planetary Science Letters 357–358 (4), 277–288.

Loomis, S.E., Russell, J.M., Heureux, A.M., D'Andrea, W.J., Sinninghe Damsté, J.S., 2014. Seasonal variability of branched glycerol dialkyl glycerol tetraethers (brGDGTs) in a temperate lake system. Geochimica et Cosmochimica Acta 144, 173–187.

Menges, J., Huguet, C., Alcañiz, J.M., Fietz, S., Sachse, D., Rosell-Melé, A., 2014. Influence of water availability in the distributions of branched glycerol dialkyl glycerol tetraether in soils of the Iberian Peninsula. Biogeosciences 11, 2571–2581.

Naafs, B.D.A., Inglis, G.N., Zheng, Y., Amesbury, M.J., Biester, H., Bindler, R., Pancost, R.D., 2017a. Introducing global peat-specific temperature and pH calibrations based on brGDGT bacterial lipids. Geochimica et Cosmochimica Acta 208, 285–301.

Naafs, B.D.A., Gallego-Sala, A.V., Inglis, G.N., Pancost, R.D., 2017b. Refining the global branched glycerol dialkyl glycerol tetraether (brGDGT) soil temperature calibration. Organic Geochemistry 106, 48–56.

Naeher, S., Peterse, F., Smittenberg, R.H., Niemann, H., Zigah, P.K., Schubert, C.J., 2014. Sources of glycerol dialkyl glycerol tetraethers (GDGTs) in catchment soils, water column and sediments of Lake Rotsee (Switzerland) - Implications for the application of GDGT-based proxies for lakes. Organic Geochemistry 66, 164–173.

Niemann, H., Stadnitskaia, A., Wirth, S.B., Gilli, A., Anselmetti, F.S., Sinninghe Damsté, J.S., Lehmann, M.F., 2012. Bacterial GDGTs in Holocene sediments and catchment soils of a high Alpine lake: application of the MBT/CBT-paleothermometer. Climate of the Past 8 (3), 889–906.

Pan, A., Yang, Q., Zhou, H., Ji, F., Wang, H., Pancost, R.D., 2016. A diagnostic GDGT signature for the impact of hydrothermal activity on surface deposits at the Southwest Indian Ridge. Organic Geochemistry 99, 90–101.

Pearson, E.J., Juggins, S., Talbot, H.M., Weckström, J., Rosén, P., Ryves, D.B., Schmidt, R., 2011. A lacustrine GDGT-temperature calibration from the Scandinavian Arctic to Antarctic: Renewed potential for the application of GDGT-paleothermometry in lakes. Geochimica et Cosmochimica Acta 75(20), 6225–6238.

Peterse, F., Kim, J.H., Schouten, S., Kristensen, D.K., Koç, N., Sinninghe Damsté, J.S., 2009a. Constraints on the application of the MBT/CBT palaeothermometer at high latitude environments (Svalbard, Norway). Organic Geochemistry 40, 692–699.

Peterse, F., Schouten, S., van der Meer, M.T.J., Sinninghe Damsté, J.S., 2009b. Distribution of branched tetraether lipids in geothermally heated soils: Implications for the MBT/CBT temperature proxy. Organic Geochemistry 40(2), 201–205.

Peterse, F., Nicol, G. W., Schouten, S., Sinninghe Damsté, J.S. 2010. Influence of soil pH on the abundance and distribution of core and intact polar lipid-derived branched GDGTs in soil. Organic Geochemistry 41(10), 1171–1175.

Peterse, F., Prins, M.A., Beets, C.J., Troelstra, S.R., Zheng, H., Gu, Z., Sinninghe Damsté, J.S., 2011. Decoupled warming and monsoon precipitation in East Asia over the last deglaciation. Earth and Planetary Science Letters 301(1–2), 256–264.

Peterse, F., van der Meer, J., Schouten, S., Weijers, J.W.H., Fierer, N., Jackson, R.B., Kim, J.H., Sinninghe Damsté, J.S., 2012. Revised calibration of the MBT-CBT paleotemperature proxy based on branched tetraether membrane lipids in surface soils. Geochimica et Cosmochimica Acta 96, 215–229.

Peterse, F., Moy, C.M., Eglinton, T.I., 2015. A laborato Biogeosciences ry experiment on the behaviour of soil-derived core and intact polar GDGTs in aquatic environments. 12(4), 933–943.

Peterse, F., Eglinton, T.I., 2017. Grain size associations of branched tetraether lipids in soils and riverbank sediments: Influence of hydrodynamic sorting processes. Frontiers in Earth Science 5, 1–8.

Réthore, G., Montier, T., LeGal, T., Delépine, P., Cammas-Marion, S., Lemiègre, L., 2007. Archaeosomes based on synthetic tetraether-like lipids as novel versatile gene delivery systems. Chemical Communications 20, 2054–2056.

Rosell, J., 1994. Mapa Geológico de España y Memoria. Escala 1:50.000, Hoja de Tremp (252).

Rueda, G., Rosell-Melé, A., Escala, M., Gyllencreutz, R., Backman, J., 2009. Comparison of instrumental and GDGT-based estimates of sea surface and air temperatures from the Skagerrak. Organic Geochemistry 40(2), 287–291.

Rull, V., Vegas-Vilarrúbia, T., 2015. Crops and weeds from the Estany de Montcortès catchment, central Pyrenees, during the last millennium: a comparison of palynological and historical records. Vegetation History and Archaeobotany 24(6), 699–710.

Sanchi, L., Ménot, G., Bard, E., 2014. Insights into continental temperatures in the northwestern Black Sea area during the Last Glacial period using branched tetraether lipids. Quaternary Science Reviews 84, 98–108.

Schlitzer R., 2010. Ocean Data View. http://odv.awi.de.

Schoon, P.L., de Kluijver, A., Middelburg, J.J., Downing, J.A., Sinninghe Damsté, J.S., Schouten, S., 2013. Influence of lake water pH and alkalinity on the distribution of core and intact polar branched glycerol dialkyl glycerol tetraethers (GDGTs) in lakes. Organic Geochemistry 60, 72–82.

Schouten, S., Hopmans, E.C., Pancost, R.D., Sinninghe Damsté, J.S., 2000. Widespread occurrence of structurally diverse tetraether membrane lipids: evidence for the ubiquitous presence of low temperature relatives of hyperthermophiles. Proceedings of the National Academy of Sciences of the United States of America 97(26), 14421–14426.

Schouten, S., van der Meer, M.T.J., Hopmans, E.C., Rijpstra, W.I.C., Reysenbach, A. L., Ward, D.M., Sinninghe Damsté, J.S., 2007. Archaeal and bacterial glycerol dialkyl glycerol tetraether lipids in hot springs of Yellowstone national park. Applied and Environmental Microbiology 73, 6181–6191.

Schouten, S., Eldrett, J., Greenwood, D.R., Harding, I., Baas, M., Sinninghe Damsté, J.S., 2008. Onset of long-term cooling of Greenland near the Eocene-Oligocene boundary as revealed by branched tetraether lipids. Geology 36(2), 147–150.

Schouten, S., Hopmans, E.C., Sinninghe Damsté, J.S., 2013. The organic geochemistry of glycerol dialkyl glycerol tetraether lipids: A review. Organic Geochemistry 54, 19–61.

Schumacher, B.A., 2002. Methods for the determination of total organic carbon (TOC) in soils and sediments. Ecological Risk Assessment Support Center. US. Environmental Protection Agency, p. 23

Servei Meteorològic de Catalunya 2011. Available at www.meteo.cat.

Shanahan, T.M., Hughen, K.A., Van Mooy, B.A.S., 2013. Temperature sensitivity of branched and isoprenoid GDGTs in Arctic lakes. Organic Geochemistry 64, 119–128.

Sinninghe Damsté, J.S., Ossebaar, J., Schouten, S., Verschuren, D., 2008. Altitudinal shifts in the branched tetraether lipid distribution in soil from Mt. Kilimanjaro (Tanzania): Implications for the MBT/CBT continental palaeothermometer. Organic Geochemistry 39, 1072–1076.

Sinninghe Damsté, J.S., Ossebaar, J., Abbas, B., Schouten, S., Verschuren, D., 2009. Fluxes and distribution of tetraether lipids in an equatorial African lake: Constraints on the application of the $TEX_{86}$ palaeothermometer and BIT index in lacustrine settings. Geochimica et Cosmochimica Acta 73(14), 4232–4249.

Sinninghe Damsté, J.S., Rijpstra, W.I.C., Hopmans, E.C., Weijers, J.W.H., Foesel, B.U., Overmann, J., Dedysh, S.N., 2011. 13,16-Dimethyl octacosanedioic acid (iso-Diabolic Acid), a common membrane-spanning lipid of Acidobacteria subdivisions 1 and 3. Applied and Environmental Microbiology 77, 4147–4154.

Sinninghe Damsté, J.S., 2016. Spatial heterogeneity of sources of branched tetraethers in shelf systems: The geochemistry of tetraethers in the Berau River delta (Kalimantan, Indonesia). Geochimica et Cosmochimica Acta 186, 13–31.

Sparkes, R.B., Doğrul S.A., Bischoff, J., Talbot, H.M., Gustafsson, S.I.P., Van Dongen, B.E., 2015. GDGT distributions on the East Siberian Arctic Shelf: Implications for organic carbon export, burial and degradation. Biogeosciences 12(12), 3753–3768.

Sumner, M.E., 1999. Handbook of soil science: pedology, soil taxonomy. CRC Press.

Sun, Q., Chu, G., Liu, M., Xie, M., Li, S., Ling, Y., Lü, H., 2011. Distributions and temperature dependence of branched glycerol dialkyl glycerol tetraethers in recent lacustrine sediments from China and Nepal. Journal of Geophysical Research: Biogeosciences 116(1), 1–12.

Thomas, G.W., 1996. Soil pH and soil acidity, in: Methods of soil analysis. Part 3 Chemical methods, SSSA Books series 5, Edited by: Sparks, D.L.  Soil Science Society of America, Madison.

Tierney, J.E., Russell, J.M., 2009. Distributions of branched GDGTs in a tropical lake system: Implications for lacustrine application of the MBT/CBT paleoproxy. Organic Geochemistry 40(9), 1032–1036.

Tierney, J.E., Russell, J.M., Eggermont, H., Hopmans, E.C., Verschuren, D., Sinninghe Damsté, J.S., 2010. Environmental controls on branched tetraether lipid distributions in tropical East African lake sediments. Geochimica et Cosmochimica Acta 74(17), 4902–4918.

Tierney, J.E., Schouten, S., Pitcher, A., Hopmans, E.C., Sinninghe Damsté, J.S., 2012. Core and intact polar glycerol dialkyl glycerol tetraethers (GDGTs) in Sand Pond, Warwick, Rhode Island (USA): Insights into the origin of lacustrine GDGTs. Geochimica et Cosmochimica Acta 77, 561–581.

Trapote, M.C., Vegas-Vilarrúbia, T., López, P., Puche, E., Gomà, J., Buchaca. T. , Cañellas-Boltà, N., Safont, E., Corella, JP. , Rull, V., 2018 Annual limnological cycle, sedimentation patterns and varve formation in Lake Montcortès (Central Pyrenees, Spain). Palaeogeography, Palaeoclimatology, Palaeoecology, doi:10.1016/j.palaeo.2018.01.046

Tyler, J.J., Nederbragt, A.J., Jones, V.J., Thurow, J.W., 2010. Assessing past temperature and soil pH estimates from bacterial tetraether membrane lipids: Evidence from the recent lake sediments of Lochnagar, Scotland. Journal of Geophysical Research G: Biogeosciences 115(1), 5-11.

Wang, H., Liu, W., Zhang, C.L., 2014. Dependence of the cyclization of branched tetraethers on soil moisture in alkaline soils from arid-subhumid China: Implications for palaeorainfall reconstructions on the Chinese Loess Plateau. Biogeosciences 11(23), 6755–6768.

Wang, H., Liu, W., Lu, H., 2016. Appraisal of branched glycerol dialkyl glycerol tetraether-based indices for North China. Organic Geochemistry 98, 118–130.

Wang, M., Zheng, Z., Man, M., Hu, J., Gao, Q. 2017a. Branched GDGT-based paleotemperature reconstruction of the last 30,000 years in humid monsoon region of Southeast China. Chemical Geology 463, 94–102.

Wang, H.Y., Liu, W.G., Lu, H.X., Zhang C.L., 2017b. Potential degradation effect on paleo-moisture proxies based on the relative abundance of archaeal vs. bacterial tetraethers in loess-paleosol sequences on the Chinese Loess Plateau. Quaternary International 2017,436, 173-180.

Warden, L., Kim, J.H., Zell, C., Vis, G.J., De Stigter, H., Bonnin, J., Sinninghe Damsté, J.S., 2016. Examining the provenance of branched GDGTs in the Tagus River drainage basin and its outflow into the Atlantic Ocean over the Holocene to determine their usefulness for paleoclimate applications. Biogeosciences 13(20), 5719–5738.

Weber, Y., Jonge, C. De, Rijpstra, W.I.C., Hopmans, E.C., Stadnitskaia, A., Schubert, C.J., Niemann, H., 2015. Identification and carbon isotope composition of a novel branched GDGT isomer in lake sediments: Evidence for lacustrine branched GDGT production. Geochimica et Cosmochimica Acta 154, 118–129.

Weber, Y., Sinninghe Damsté, J.S., Hopmans, E.C., Lehmann, M.F., Niemann, H., 2017. Incomplete recovery of intact polar glycerol dialkyl glycerol tetraethers from lacustrine suspended biomass. Limnology and Oceanography: Methods (Cl)15, 782–793.

Weijers, J.W.H., Schouten S., Hopmans, E.C., Geenevasen, J., David, O.R., Coleman, J.M., Pancost, R.D., Sinninghe Damsté, J.S., 2006. Membrane lipids of mesophilic anaerobic bacteria thriving in peats have typical archaeal traits. Environmental Microbiology 8 (4), 648-657.

Weijers, J.W.H., Schouten, S., van den Donker, J.C., Hopmans, E.C., Sinninghe Damsté, J.S., 2007. Environmental controls on bacterial tetraether membrane lipid distribution in soils. Geochimica et Cosmochimica Acta 71(3), 703–713.

Weijers, J.W.H., Panoto, E., van Bleijswijk, J., Schouten, S., Rijpstra, W.I.C., Balk, M., Stams, A.J.M., Sinninghe Damsté, J.S., 2009. Constraints on the biological source(s) of the orphan branched tetraether membrane lipids. Geomicrobiology Journal 26, 402-414

Weijers, J.W.H., Wiesenberg, G.L.B., Bol, R., Hopmans, E.C., Pancost, R.D., 2010. Carbon isotopic composition of branched tetraether membrane lipids in soils suggest a rapid turnover and a heterotrophic life style of their source organism(s). Biogeosciences 7(9), 2959–2973.

Weijers, J.W.H., Bernhardt, B., Peterse, F., Werne, J.P., Dungait, J.A.J., Schouten, S., Sinninghe Damsté, J.S., 2011. Absence of seasonal patterns in MBT-CBT indices in mid-latitude soils. Geochimica et Cosmochimica Acta 75, 3179–3190.

Weijers, J.W.H., Schefuß, E., Kim, J.H., Sinninghe Damsté, J.S., Schouten, S., 2014. Constraints on the sources of branched tetraether membrane lipids in distal marine sediments. Organic Geochemistry 72, 14–22.

Wu, X., Dong, H., Zhang, C.L., Liu, X., Hou, W., Zhang, J., Jiang, H., 2013. Evaluation of glycerol dialkyl glycerol tetraether proxies for reconstruction of the paleo-environment on the Qinghai-Tibetan Plateau. Organic Geochemistry 61, 45–56.

Xiao, W., Wang, Y., Zhou, S., Hu, L., Yang, H., Xu, Y., 2016. Ubiquitous production of branched glycerol dialkyl glycerol tetraethers (brGDGTs) in global marine environments: A new source indicator for brGDGTs. Biogeosciences 13(20), 5883–5894.

Yamamoto, M., Shimamoto, A., Fukuhara, T., Tanaka, Y., 2016. Source, settling and degradation of branched glycerol dialkyl glycerol tetraethers in the marine water column. Geochimica et Cosmochimica Acta 191, 239–254.

Yang, H., Ding, W., Zhang, C.L., Wu, X., Ma, X., He, G., Xie, S., 2011. Occurrence of tetraether lipids in stalagmites: Implications for sources and GDGT-based proxies. Organic Geochemistry 42(1), 108–115.

Yang, H., Pancost, R.D., Dang, X., Zhou, X., Evershed, R.P., Xiao, G., Xie, S., 2014a. Correlations between microbial tetraether lipids and environmental variables in Chinese soils: Optimizing the paleo-reconstructions in semi-arid and arid regions. Geochimica et Cosmochimica Acta 126, 49–69.

Yang, H., Pancost, R.D., Tang, C., Ding, W., Dang, X., Xie, S., 2014b. Distributions of isoprenoid and branched glycerol dialkanol diethers in Chinese surface soils and a loess paleosol sequence: Implications for the degradation of tetraether lipids. Organic Geochemistry 66, 70–79.

Yang, H., Lü, X., Ding, W., Lei, Y., Dang, X., Xie, S., 2015. The 6-methyl branched tetraethers significantly affect the performance of the methylation index (MBT') in soils from an altitudinal transect at Mount Shennongjia. Organic Geochemistry 82, 42–53.

Zech, R., Gao, L., Tarozo, R., Huang, Y., 2012. Branched glycerol dialkyl glycerol tetraethers in Pleistocene loess-paleosol sequences: Three case studies. Organic Geochemistry 53, 38–44.

Zell, C., Kim, J.H., Hollander, D., Lorenzoni, L., Baker, P., Silva, C.G., Sinninghe Damsté, J.S., 2014a. Sources and distributions of branched and isoprenoid tetraether lipids on the Amazon shelf and fan: Implications for the use of GDGT-based proxies in marine sediments. Geochimica et Cosmochimica Acta 139, 293–312.

Zell, C., Kim, J.H., Balsinha, M., Dorhout, D.J.C., Fernandes, C., Baas, M., Sinninghe Damsté, J.S., 2014b. Transport of branched tetraether lipids from the Tagus River basin to the coastal ocean of the Portuguese margin: Consequences for the interpretation of the MBT'/CBT paleothermometer. Biogeosciences 11(19), 5637-5655.

Zhang, C.L., Wang, J., Wei, Y., Zhu, C., Huang, L., Dong, H., 2012. Production of branched tetraether lipids in the lower Pearl River and estuary: Effects of extraction methods and impact on brGDGT proxies. Frontiers in Microbiology 2, 1–18.

Zheng, F., Zhang, C., Chen, Y., Li, F., Ma, C., Pu, Y., Liu, W., 2016. Branched tetraether lipids in Chinese soils: Evaluating the fidelity of MBT/CBT proxies as paleoenvironmental proxies. Science China Earth Sciences 59, 1353–1367.

Zhu, C., Weijers, J.W.H., Wagner, T., Pan, J.M., Chen, J.F., Pancost, R.D., 2011. Sources and distributions of tetraether lipids in surface sediments across a large river-dominated continental margin. Organic Geochemistry 42(4), 376–386.

Zink, K.G., Vandergoes, M.J., Mangelsdorf, K., Dieffenbacher-Krall, A.C., Schwark, L. 2010. Application of bacterial glycerol dialkyl glycerol tetraethers (GDGTs) to develop modern and past temperature estimates from New Zealand lakes. Organic Geochemistry 41(9), 1060–1066.

Zink, K.G., Vandergoes, M.J., Bauersachs, T., Newnham, R.M., Rees, A.B.H., Schwark, L., 2016. A refined paleotemperature calibration for New Zealand limnic environments using differentiation of branched glycerol dialkyl glycerol tetraether (brGDGT) sources. Journal of Quaternary Science 31(7), 823–835.

**Figure**

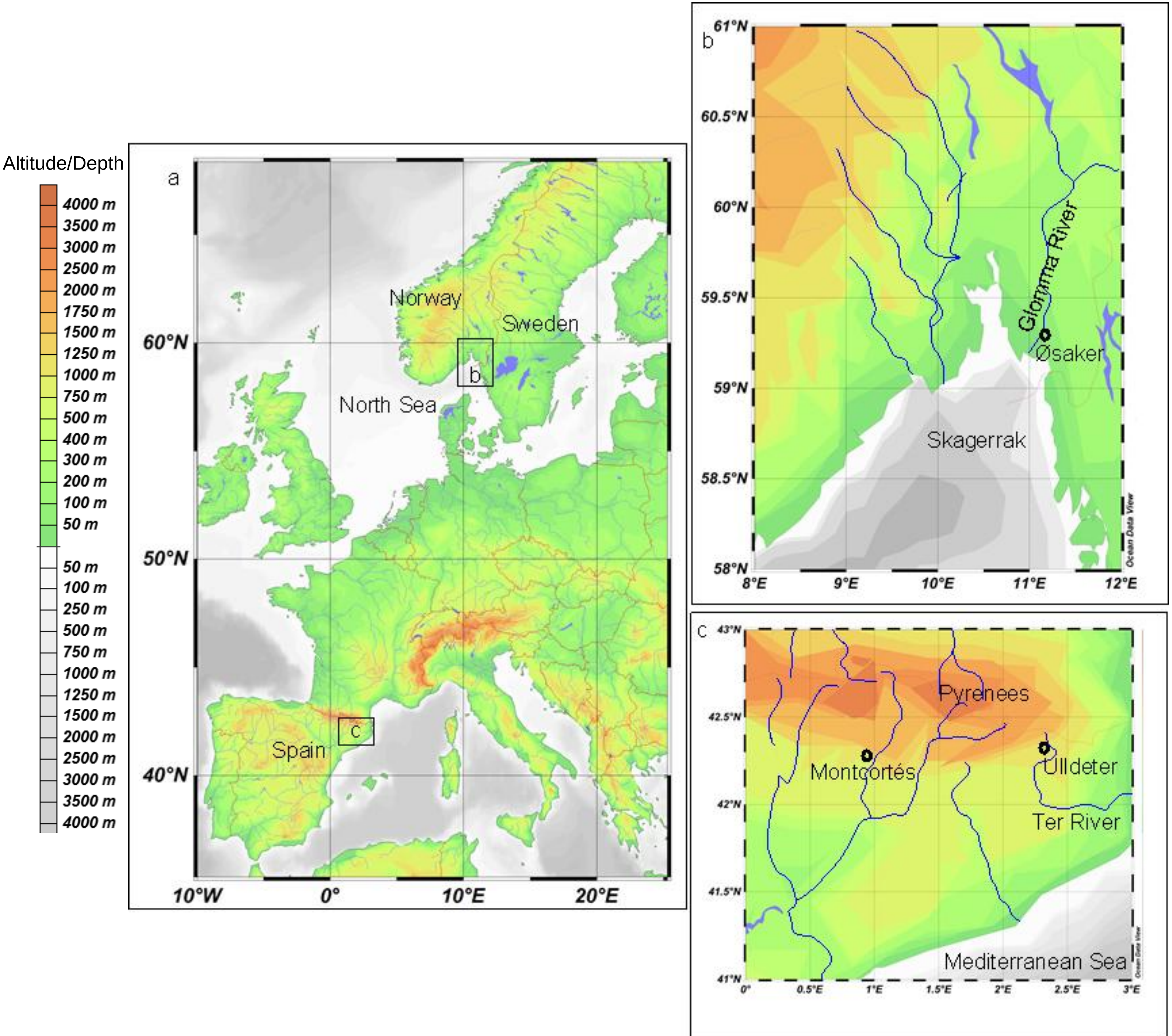
Altitude/Depth
4000 m
3500 m
3000 m
2500 m
2000 m
1750 m
1500 m
1250 m
1000 m
750 m
500 m
400 m
300 m
200 m
100 m
50 m
50 m
100 m
250 m
500 m
750 m
1000 m
1250 m
1500 m
2000 m
2500 m
3000 m
3500 m
4000 m
a
Norway
Sweden
North Sea
b
c
Spain
60°N
50°N
40°N
10°W
0°
10°E
20°E
b
61°N
60.5°N
60°N
59.5°N
59°N
58.5°N
58°N
8°E
9°E
10°E
11°E
12°E
Glomma River
Øsaker
Skagerrak
Ocean Data View
C
43°N
42.5°N
42°N
41.5°N
41°N
0°
0.5°E
1°E
1.5°E
2°E
2.5°E
3°E
Pyrenees
Montcortés
Ulldeter
Ter River
Mediterranean Sea
Ocean Data View

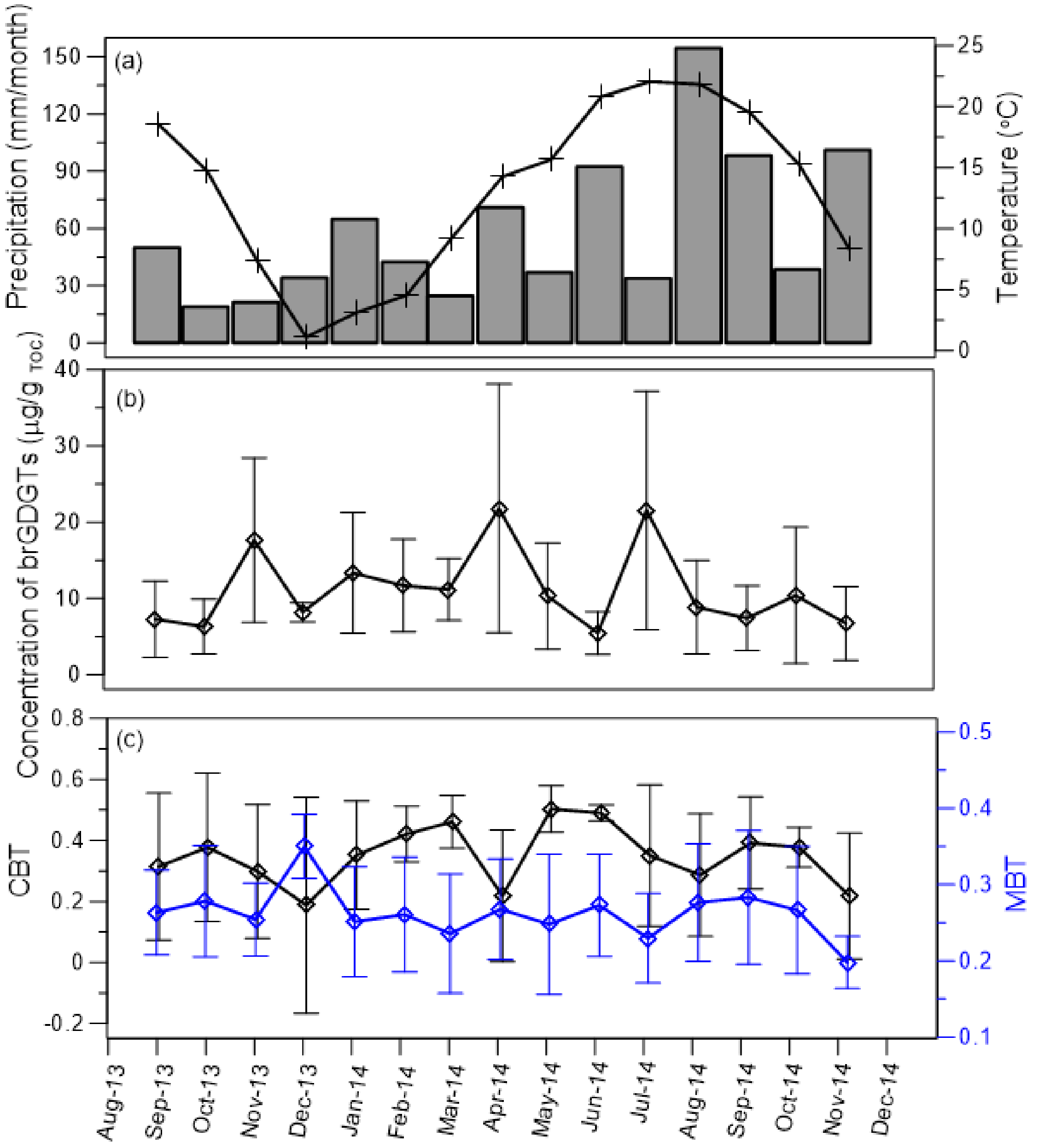

(a)
Precipitation (mm/month)
0
30
60
90
120
150
Temperature (°C)
0
5
10
15
20
25
(b)
Concentration of brGDGTs (μg/g TOC)
0
10
20
30
40
(c)
CBT
-0.2
0
0.2
0.4
0.6
0.8
MBT
0.1
0.2
0.3
0.4
0.5
Aug-13
Sep-13
Oct-13
Nov-13
Dec-13
Jan-14
Feb-14
Mar-14
Apr-14
May-14
Jun-14
Jul-14
Aug-14
Sep-14
Oct-14
Nov-14
Dec-14

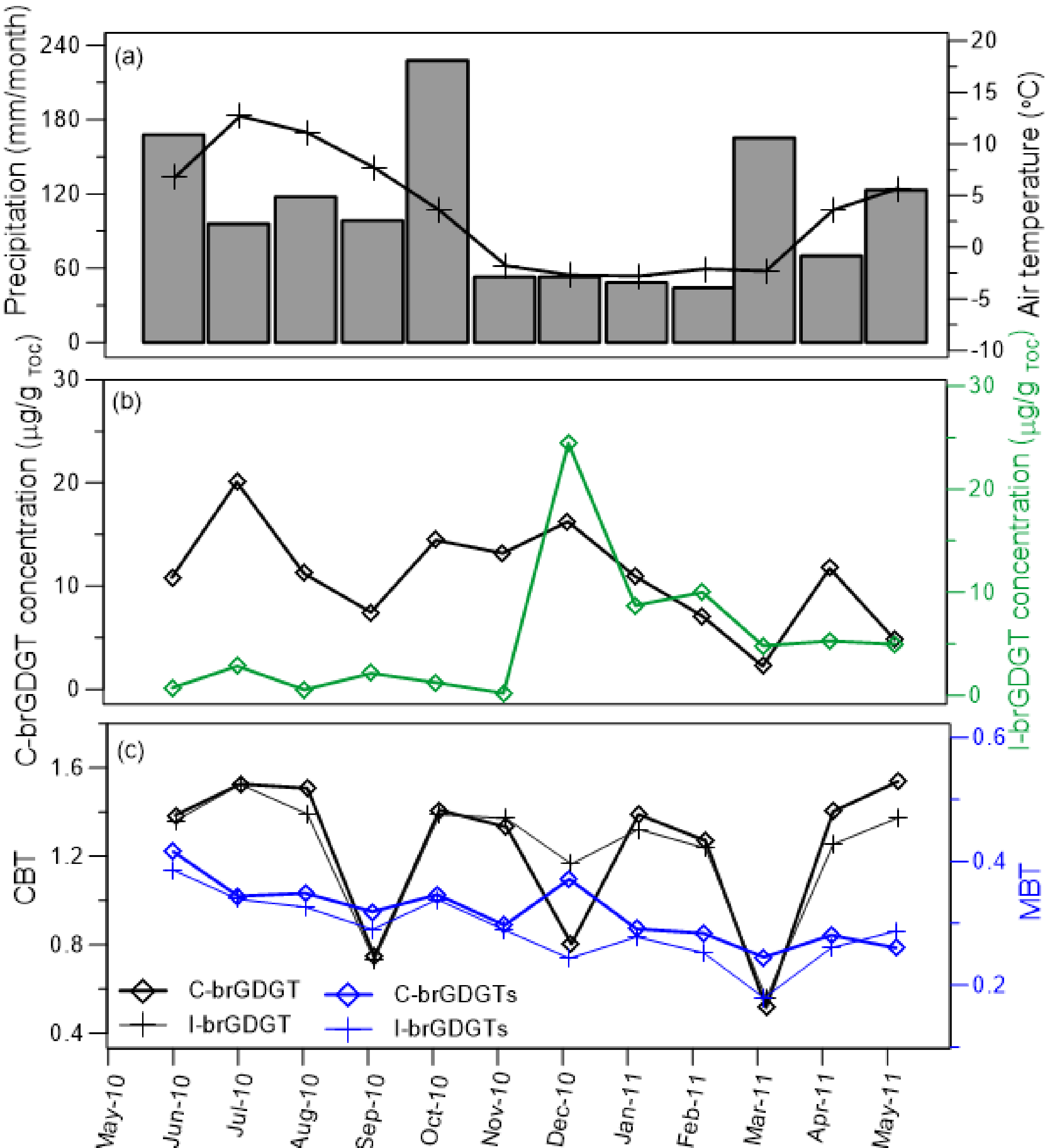
(a)
Precipitation (mm/month)
240
180
120
60
0
Air temperature (°C)
20
15
10
5
0
-5
-10
(b)
C-brGDGT concentration (μg/g TOC)
30
20
10
0
I-brGDGT concentration (μg/g TOC)
30
20
10
0
(c)
CBT
1.6
1.2
0.8
0.4
MBT
0.6
0.4
0.2
C-brGDGT
I-brGDGT
C-brGDGTs
I-brGDGTs
May-10
Jun-10
Jul-10
Aug-10
Sep-10
Oct-10
Nov-10
Dec-10
Jan-11
Feb-11
Mar-11
Apr-11
May-11

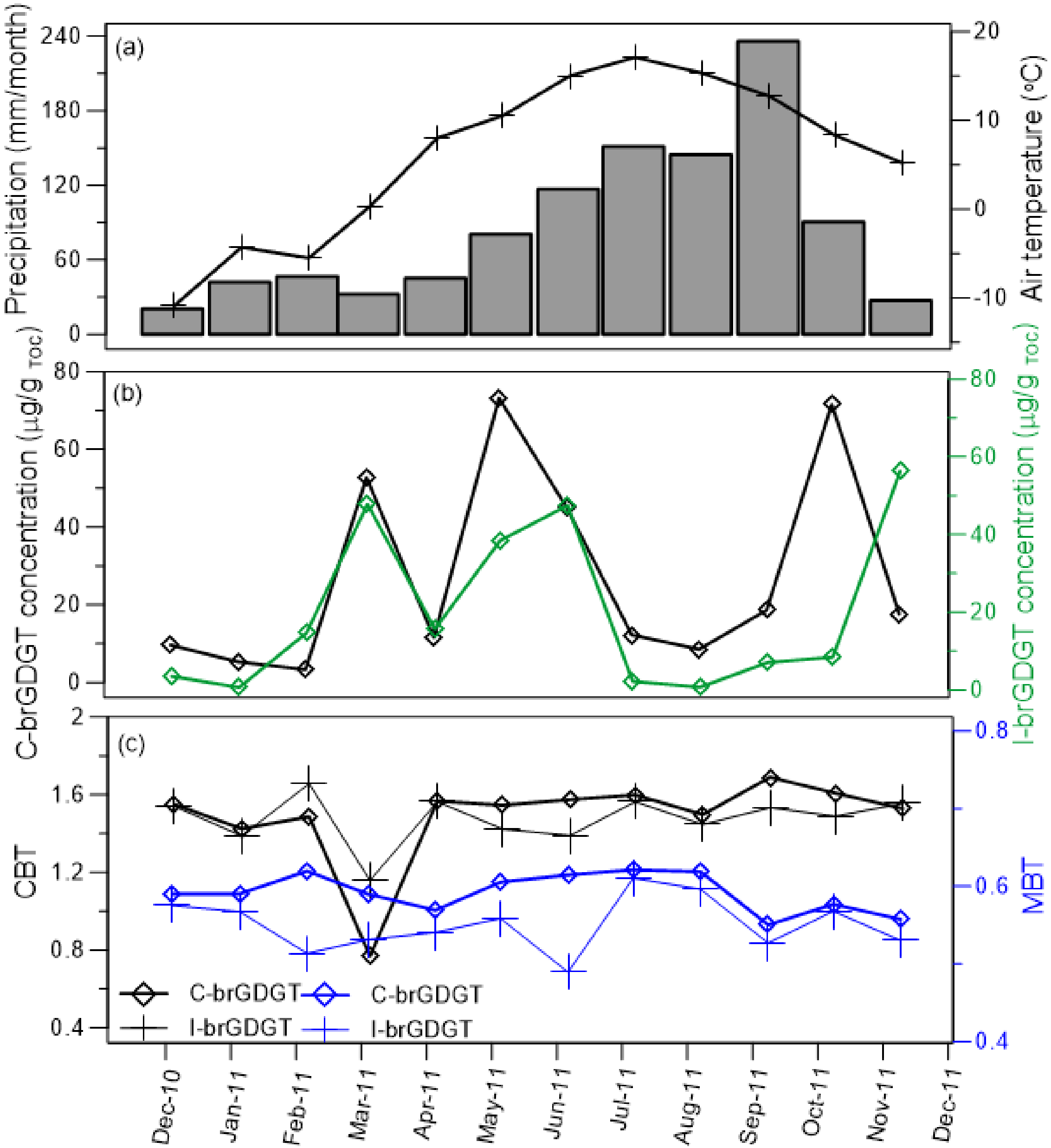
(a)
Precipitation (mm/month)
0
60
120
180
240
Air temperature (°C)
-10
0
10
20
(b)
C-brGDGT concentration (µg/g TOC)
0
20
40
60
80
I-brGDGT concentration (µg/g TOC)
0
20
40
60
80
(c)
CBT
0.4
0.8
1.2
1.6
2
MBT
0.4
0.6
0.8
C-brGDGT
I-brGDGT
C-brGDGT
I-brGDGT
Dec-10
Jan-11
Feb-11
Mar-11
Apr-11
May-11
Jun-11
Jul-11
Aug-11
Sep-11
Oct-11
Nov-11
Dec-11

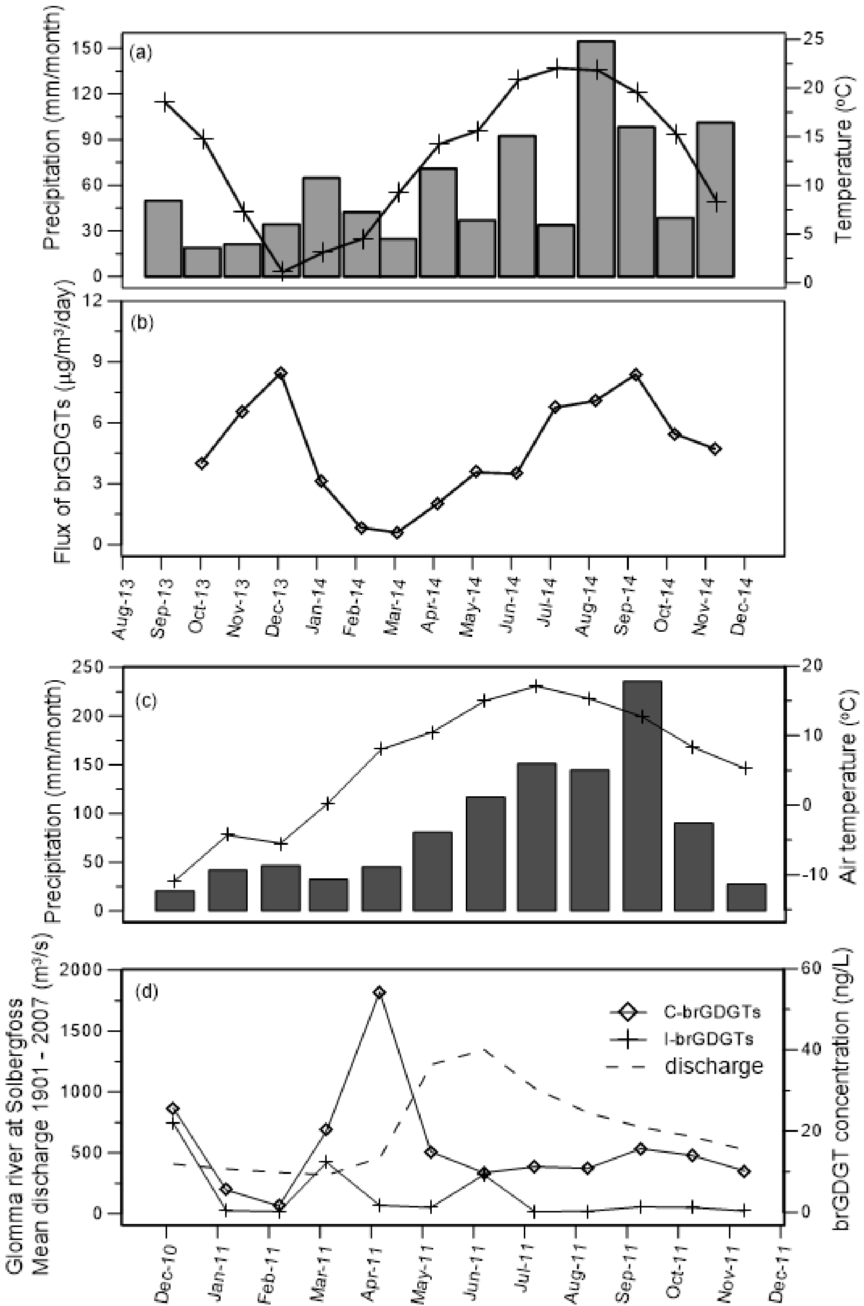
(a)
Precipitation (mm/month)
150
120
90
60
30
0
Temperature (ºC)
25
20
15
10
5
0
(b)
Flux of brGDGTs (µg/m³/day)
12
9
6
3
0
Aug-13
Sep-13
Oct-13
Nov-13
Dec-13
Jan-14
Feb-14
Mar-14
Apr-14
May-14
Jun-14
Jul-14
Aug-14
Sep-14
Oct-14
Nov-14
Dec-14
(c)
Precipitation (mm/month)
250
200
150
100
50
0
Air temperature (ºC)
20
10
0
-10
(d)
Glomma river at Solbergfoss
Mean discharge 1901 - 2007 (m³/s)
2000
1500
1000
500
0
brGDGT concentration (ng/L)
60
40
20
0
C-brGDGTs
I-brGDGTs
discharge
Dec-10
Jan-11
Feb-11
Mar-11
Apr-11
May-11
Jun-11
Jul-11
Aug-11
Sep-11
Oct-11
Nov-11
Dec-11

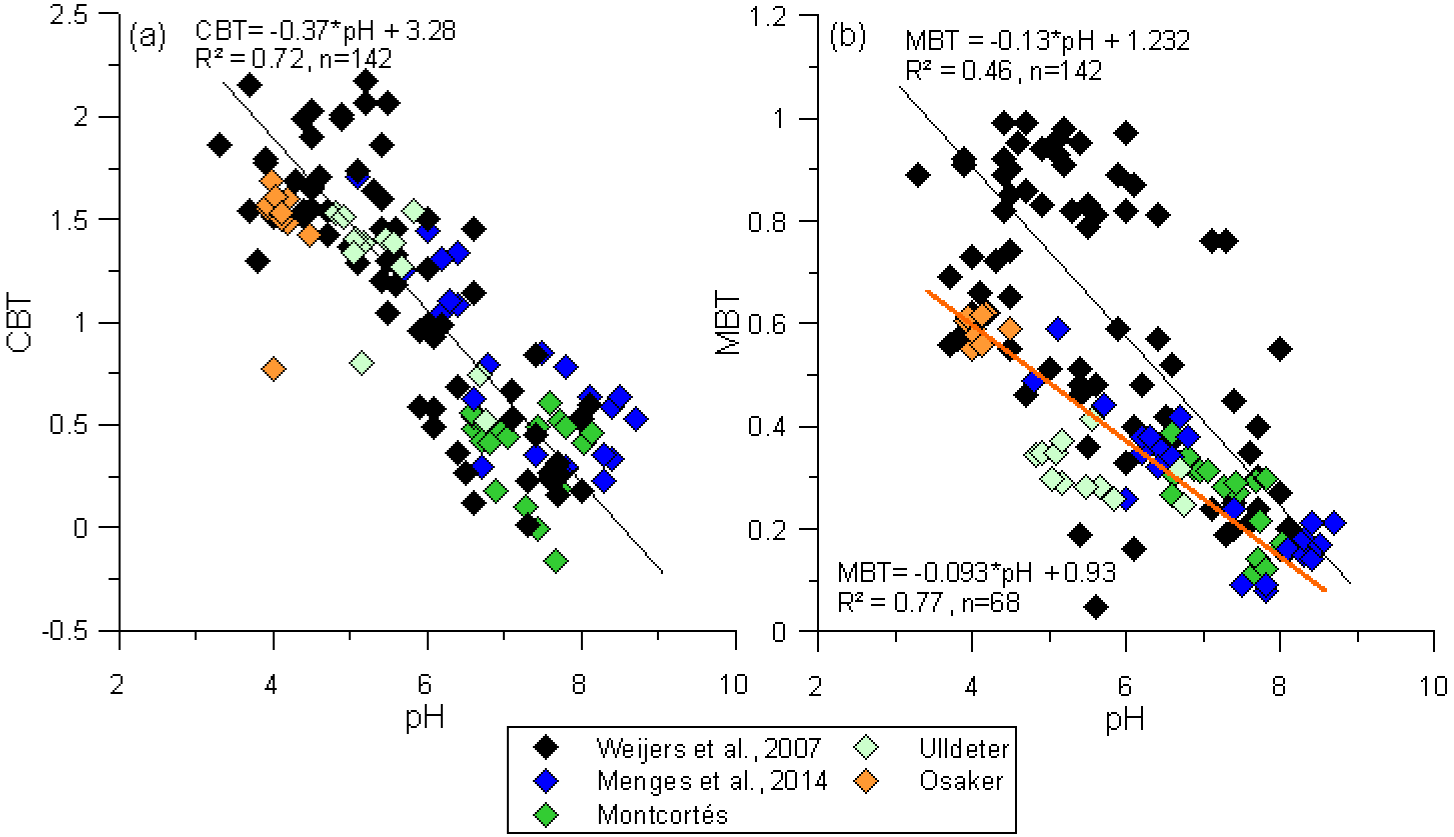
(a)
CBT= -0.37*pH + 3.28
R² = 0.72, n=142
CBT
2.5
2
1.5
1
0.5
0
-0.5
2
4
6
8
10
pH
(b)
MBT = -0.13*pH + 1.232
R² = 0.46 , n=142
MBT= -0.093*pH +0.93
R² = 0.77 , n=68
MBT
1.2
1
0.8
0.6
0.4
0.2
0
2
4
6
8
10
pH
◆ Weijers et al., 2007
◆ Menges et al., 2014
◆ Montcortés
◇ Ulldeter
◆ Osaker

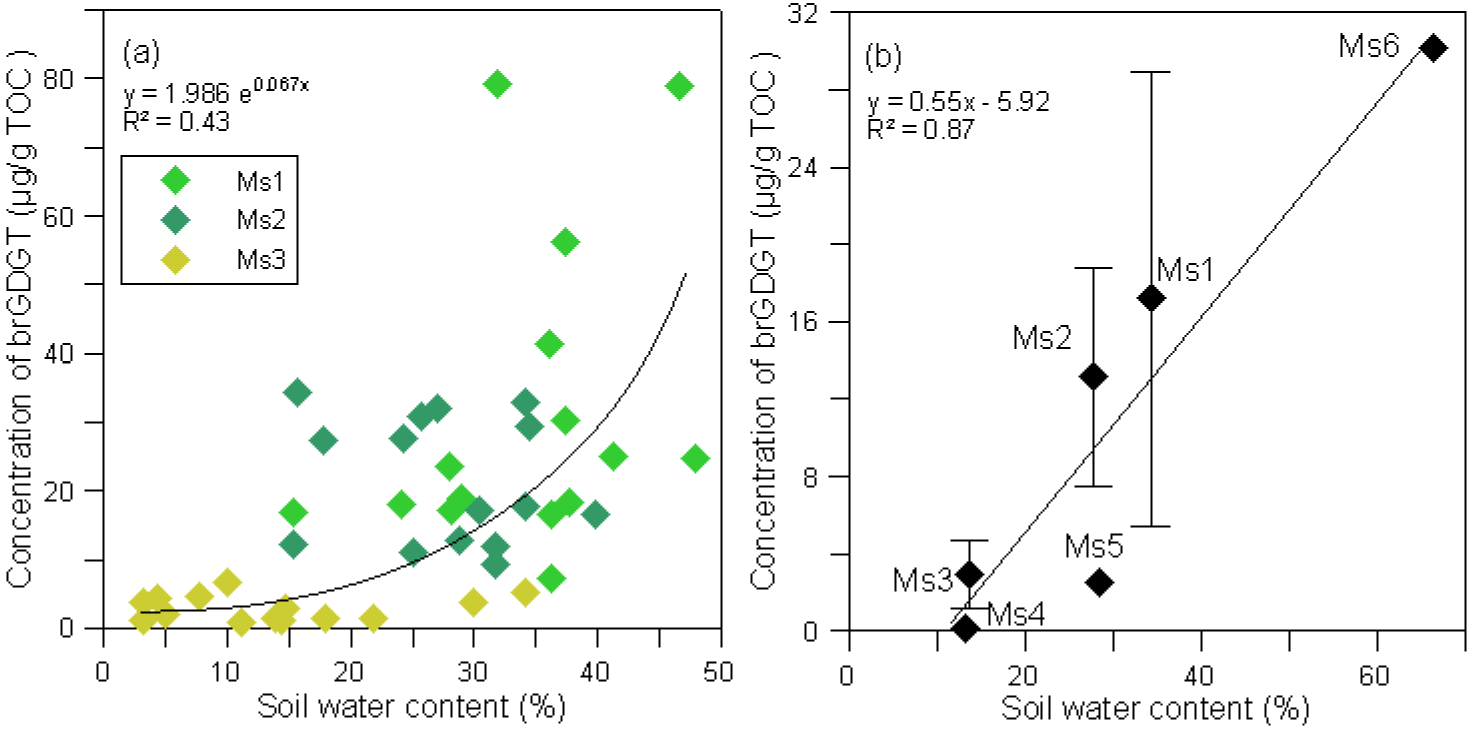
(a)
y = 1.986 e$^{0.067x}$
R² = 0.43
Ms1
Ms2
Ms3
Concentration of brGDGT (μg/g TOC )
0
20
40
60
80
0
10
20
30
40
50
Soil water content (%)
(b)
y = 0.55x - 5.92
R² = 0.87
Ms6
Ms1
Ms2
Ms3
Ms4
Ms5
Concentration of brGDGT (μg/g TOC )
0
8
16
24
32
0
20
40
60
Soil water content (%)

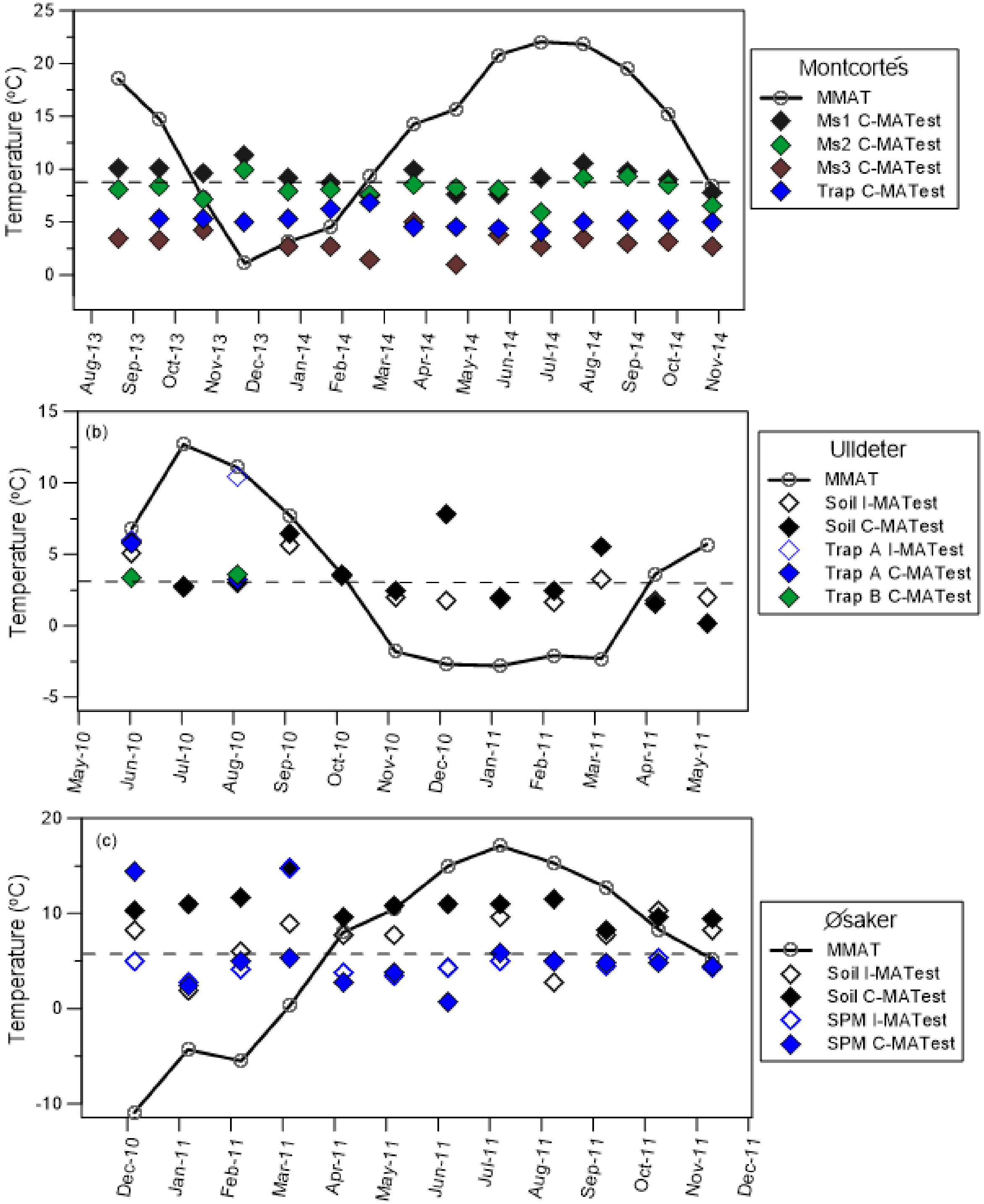
25
20
15
10
5
0
Temperature (ºC)
Aug-13
Sep-13
Oct-13
Nov-13
Dec-13
Jan-14
Feb-14
Mar-14
Apr-14
May-14
Jun-14
Jul-14
Aug-14
Sep-14
Oct-14
Nov-14
Montcortés
MMAT
Ms1 C-MATest
Ms2 C-MATest
Ms3 C-MATest
Trap C-MATest
15
10
5
0
-5
(b)
Temperature (ºC)
May-10
Jun-10
Jul-10
Aug-10
Sep-10
Oct-10
Nov-10
Dec-10
Jan-11
Feb-11
Mar-11
Apr-11
May-11
Ulldeter
MMAT
Soil I-MATest
Soil C-MATest
Trap A I-MATest
Trap A C-MATest
Trap B C-MATest
20
10
0
-10
(c)
Temperature (ºC)
Dec-10
Jan-11
Feb-11
Mar-11
Apr-11
May-11
Jun-11
Jul-11
Aug-11
Sep-11
Oct-11
Nov-11
Dec-11
Øsaker
MMAT
Soil I-MATest
Soil C-MATest
SPM I-MATest
SPM C-MATest